

CALET

Calorimetric
Electron
Telescope



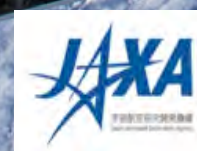
Pier Simone Marrocchesi

University of Siena & INFN-Pisa

for the CALET Collaboration

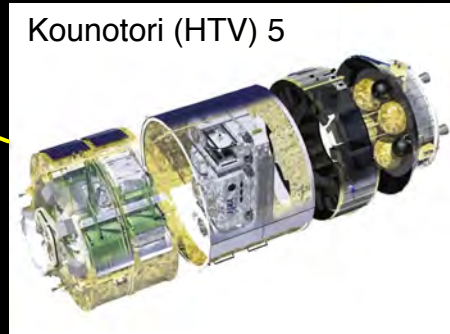
NextGapes - 2019

Moscow, 2019 June 21-22





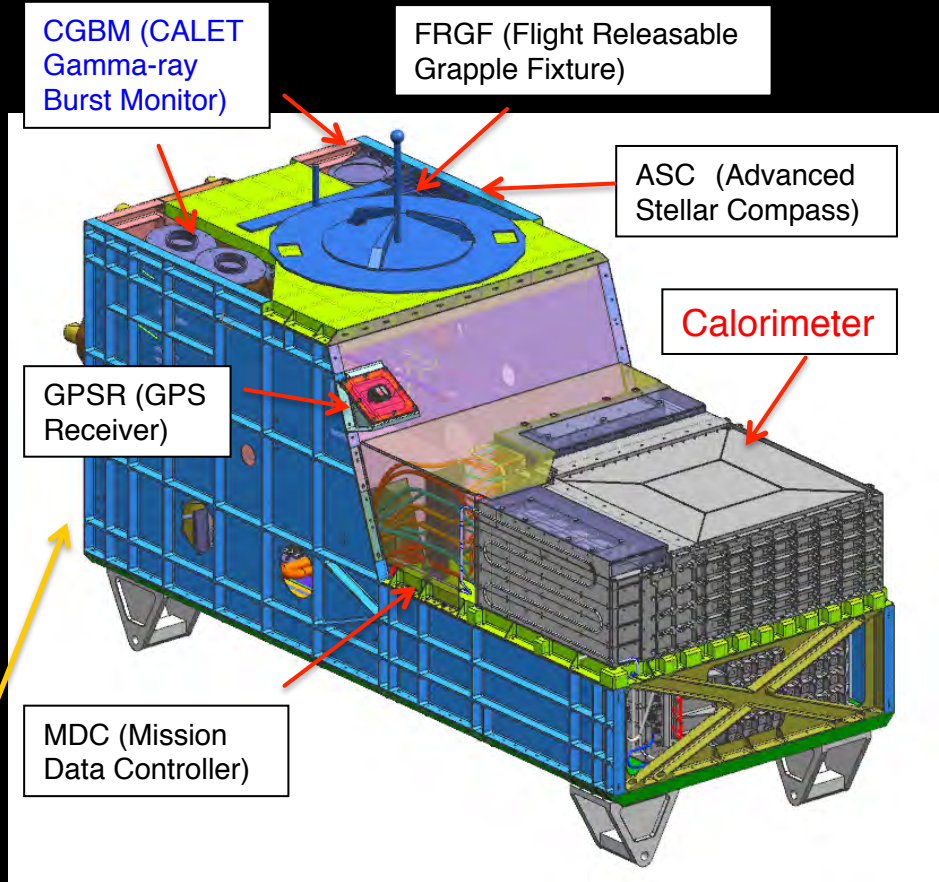
CALET Payload



Kounotori (HTV) 5

Launched on Aug. 19th, 2015 by the Japanese H2-B rocket

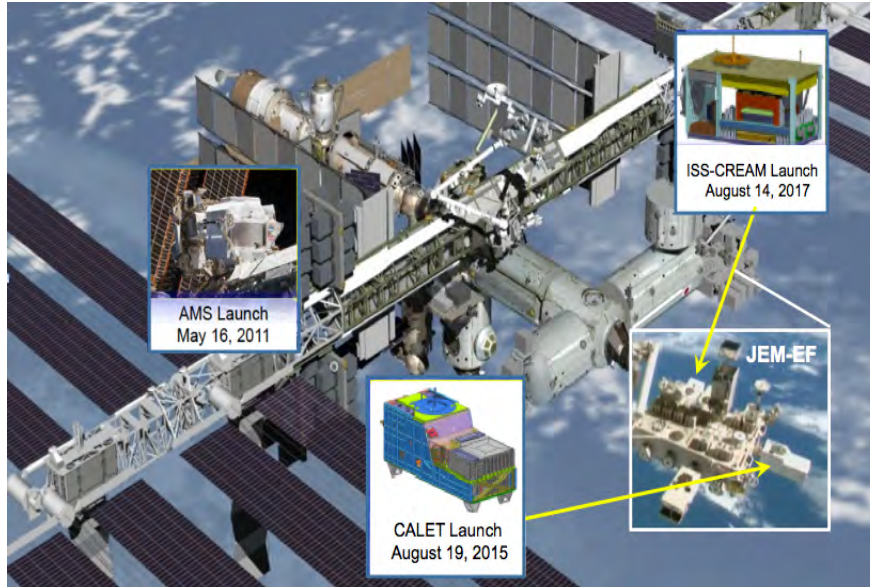
Emplaced on port #9 of JEM-EF (Japanese Experiment Module Exposed Facility) on Aug. 25th



- **Mass:** 612.8 kg JEM Standard Payload
- **Size:** 1850mm (L) × 800mm (W) × 1000mm (H)
- **Power:** 507 W (max)
- **Telemetry:** Medium 600 kbps (6.5GB/day)



Cosmic Ray Observations aboard the ISS and CALET program



Main CALET science objectives:

- ✧ **Electron observation** in 1 GeV - 20 TeV range. Design optimized for electron detection: high energy resolution and large e/p separation power + e.m. shower containment. Detailed study of spectral shape. **Search for Dark Matter and Nearby Sources**
- ✧ **Observation of cosmic-ray nuclei** in the energy region from 10 GeV to 1 PeV. **Unravelling the CR acceleration and propagation mechanism(s)**
- ✧ Detection of **transient phenomena** in space **Gamma-ray bursts, e.m. GW counterparts, Solar flares, Space Weather**

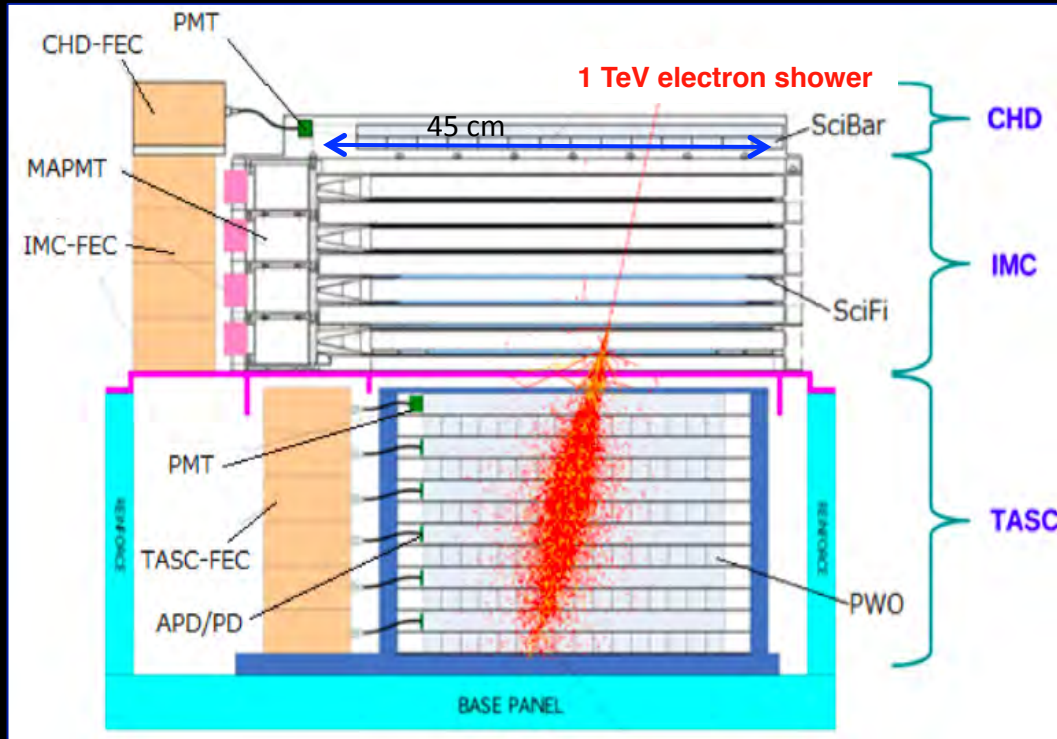
Scientific Objectives	Observation Targets	Energy Range
CR Origin and Acceleration	Electron spectrum Individual spectra of elements from proton to Fe Ultra Heavy Ions ($26 < Z \leq 40$) Gamma-rays (Diffuse + Point sources)	1 GeV - 20 TeV 10 GeV - 1000 TeV > 600 MeV/n 1 GeV - 1 TeV
Galactic CR Propagation	B/C and sub-Fe/Fe ratios	Up to some TeV/n
Nearby CR Sources	Electron spectrum	100 GeV - 20 TeV
Dark Matter	Signatures in electron/gamma-ray spectra	100 GeV - 20 TeV
Solar Physics	Electron flux (1 GeV-10 GeV)	< 10 GeV
Gamma-ray Transients	Gamma-rays and X-rays	7 keV - 20 MeV



CALET instrument in a nutshell

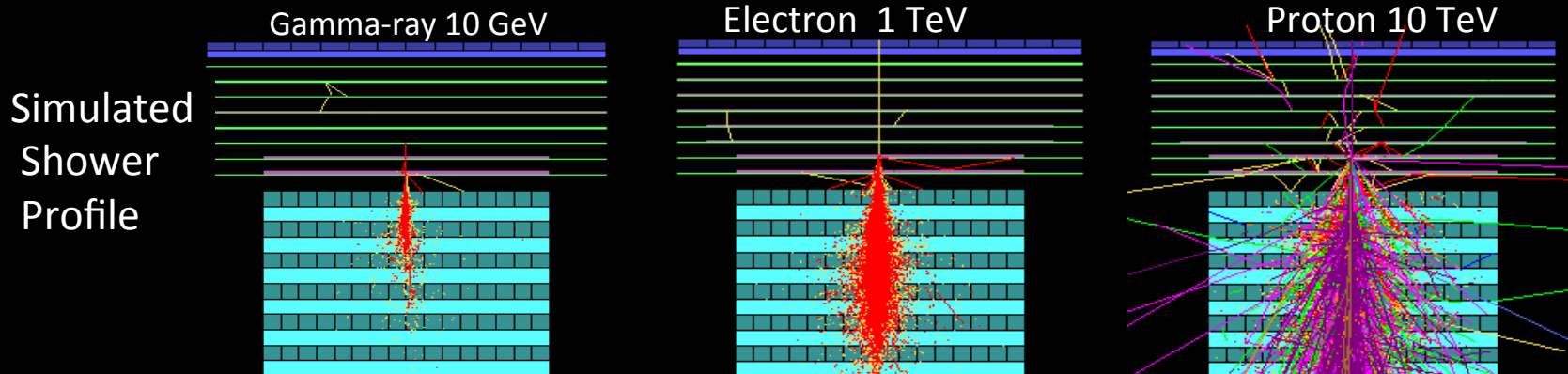
Field of view: ~ 45 degrees (from the zenith)

Geometrical Factor: $\sim 1,040 \text{ cm}^2\text{sr}$ (for electrons)



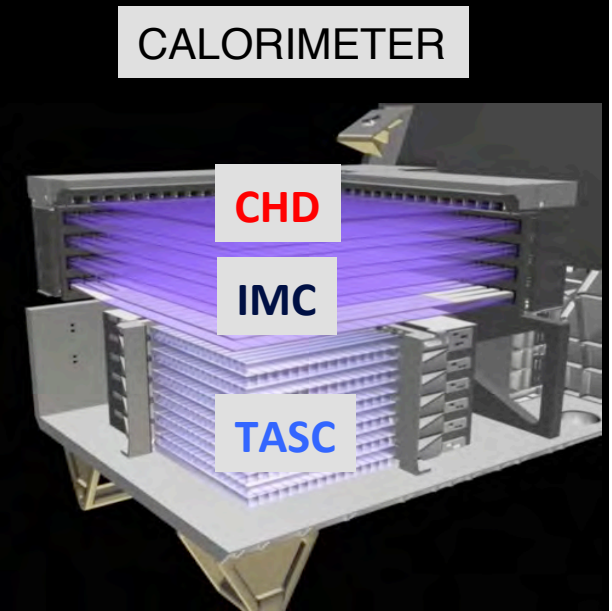
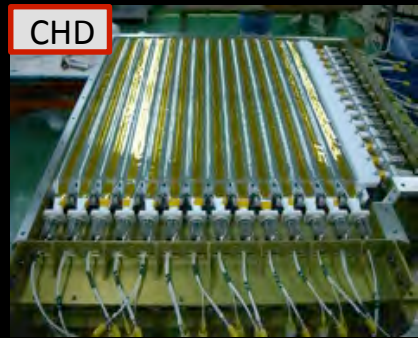
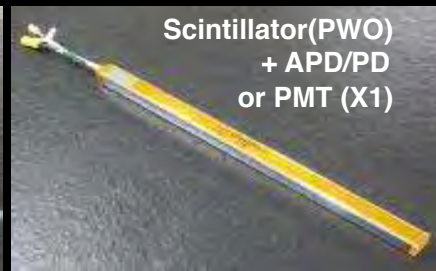
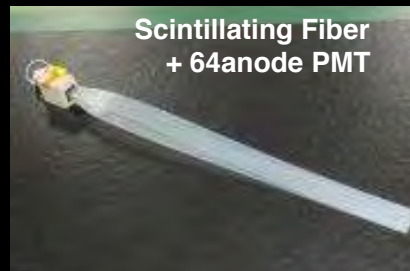
CALET: a unique set of key instruments

- **CHD**: a dedicated **charge detector + multiple dE/dx sampling in the IMC** allow the **identification of individual nuclear species** (charge resolution $\sim 0.15\text{-}0.3 e$).
- **IMC**: **high granularity (1mm) imaging pre-shower calorimeter** to accurately reconstruct the **arrival direction** of incident particles ($\sim 0.1^\circ$) and the **starting point** of electro-magnetic showers.
 SciFi + Tungsten absorbers: $3 X_0$ ($= 0.2 X_0 \times 5 + 1.0 X_0 \times 2$)
- **TASC**: thick ($27 X_0$) homogeneous PWO calorimeter allowing to extend electron measurements into the TeV energy region with $\sim 2\%$ **energy resolution**.
- **Combined** ($30 X_0, 1.2 \lambda_1$) they **separate electrons** from the abundant protons (rejection $> 10^5$).





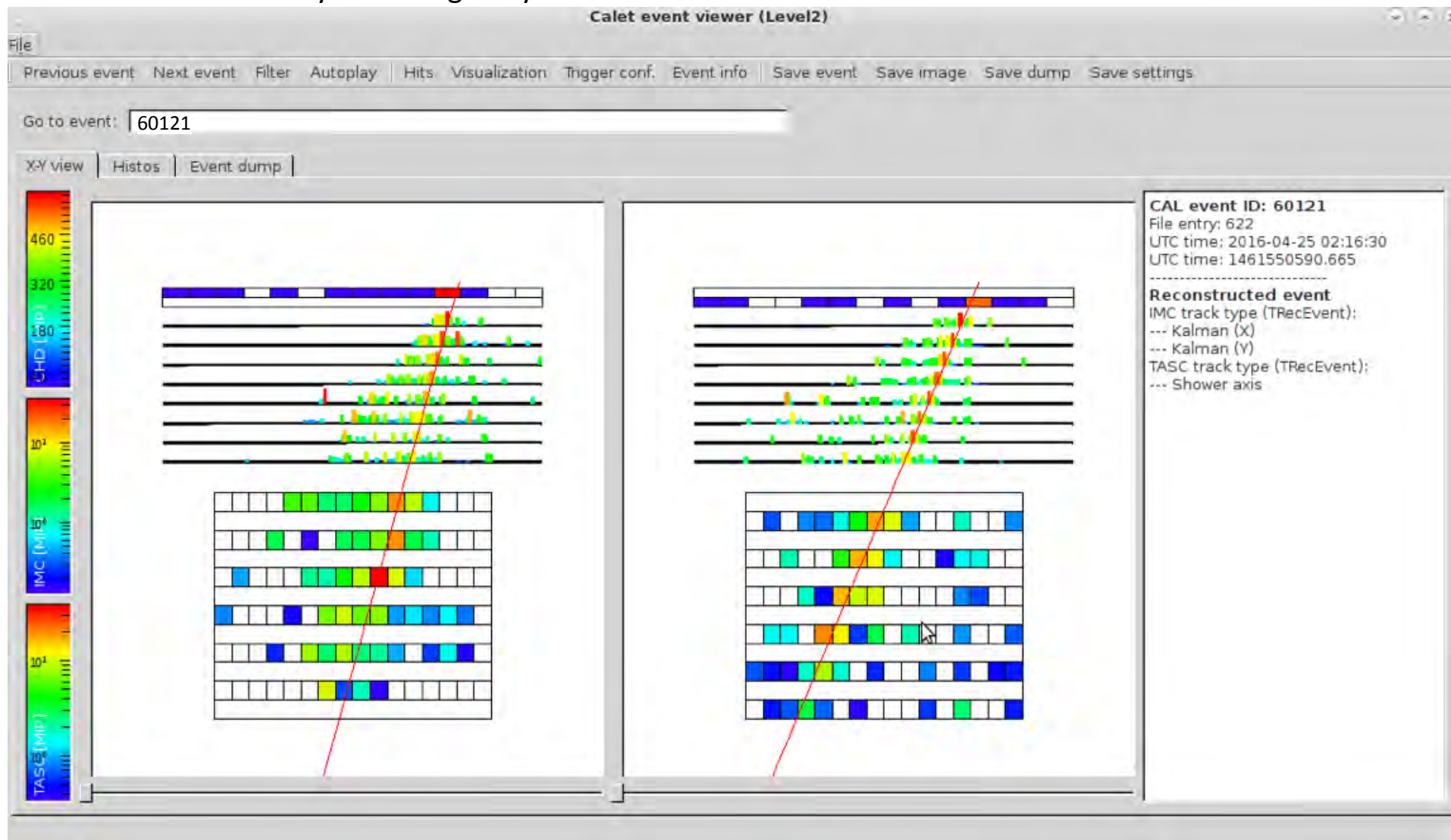
CALET Instrument overview



	CHD (Charge Detector)	IMC (Imaging Calorimeter)	TASC (Total Absorption Calorimeter)
Measure	Charge (Z=1-40)	Tracking , Particle ID	Energy, e/p Separation
Geometry (Material)	Plastic Scintillators: 28 paddles 14 paddles x 2 layers (X,Y) Paddle Size: 32 x 10 x 450 mm ³	Scintillating Fibers: 448 x 16 layers (X,Y) Scifi size: 1 x 1 x 448 mm ³ 7 Tungsten layers : 0.2X ₀ x 5 + 1X ₀ x 2 Total Thickness: 3 X ₀	PWO logs: 16 x 12 layers (x,y): 192 logs log size: 19 x 20 x 326 mm ³ Total Thickness: 27 X ₀ , ~1.2 λ _i
Readout	PMT+CSA	64-anode PMT+ ASIC	APD/PD+CSA PMT+CSA (for Trigger)@top layer

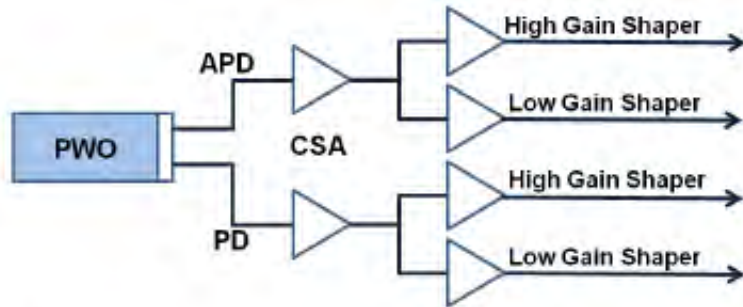
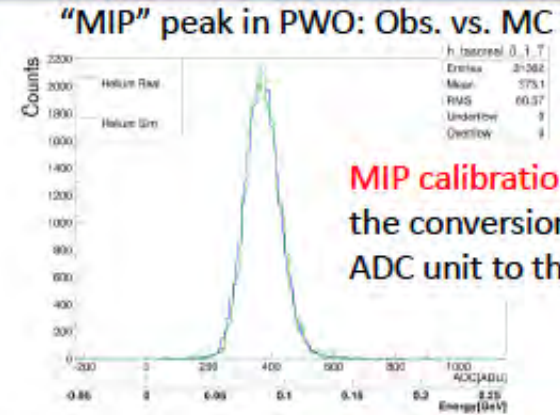
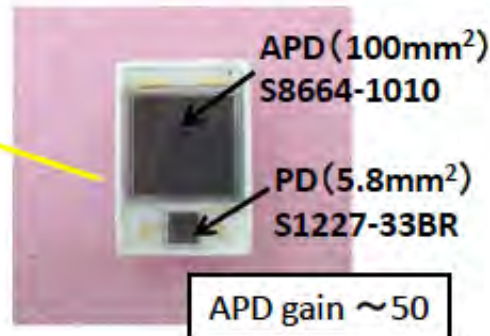
✧ CALET **tracking** takes advantage of the IMAGING capabilities of IMC thanks to its granularity of **1 mm with Sci-fibers readout individually**

Example: A **multi-prong event** due to an interaction of the primary particle in the CHD is very well imaged by the IMC.





Energy Measurement in a wide dynamic range 1-10⁶ MIPs

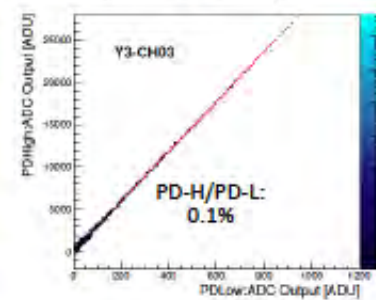
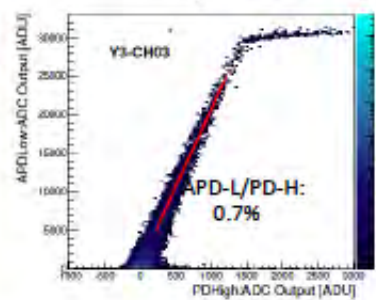
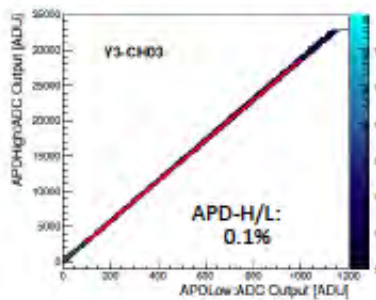


The whole dynamic range was calibrated by **UV laser irradiation** on ground :
 1) The linearity of each gain range is confirmed in the range of 1.4-2.5 %.
 2) Each channel covers from 1 MIP to 10⁶ MIPs.

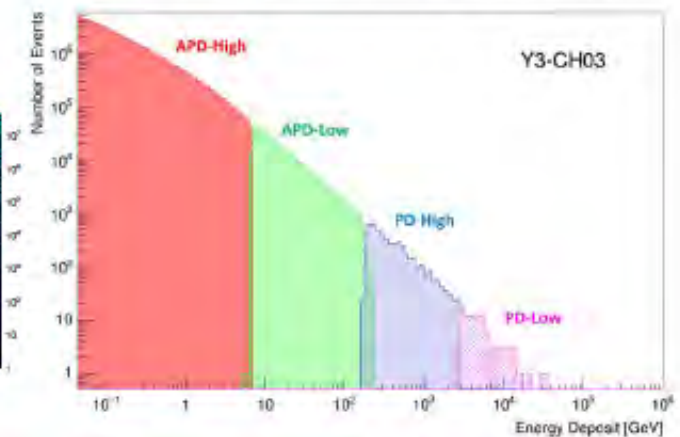
APD-H	APD-L	PD-H	PD-L
1.4%	1.5%	2.5%	2.2%

The correlation between adjacent gain ranges is calibrated by using **in-flight data** in each channel.

APD-H APD-L	APD-L PD-H	PD-H PD-L
0.1%	0.7%	0.1%



Example of energy distribution in one PWO log



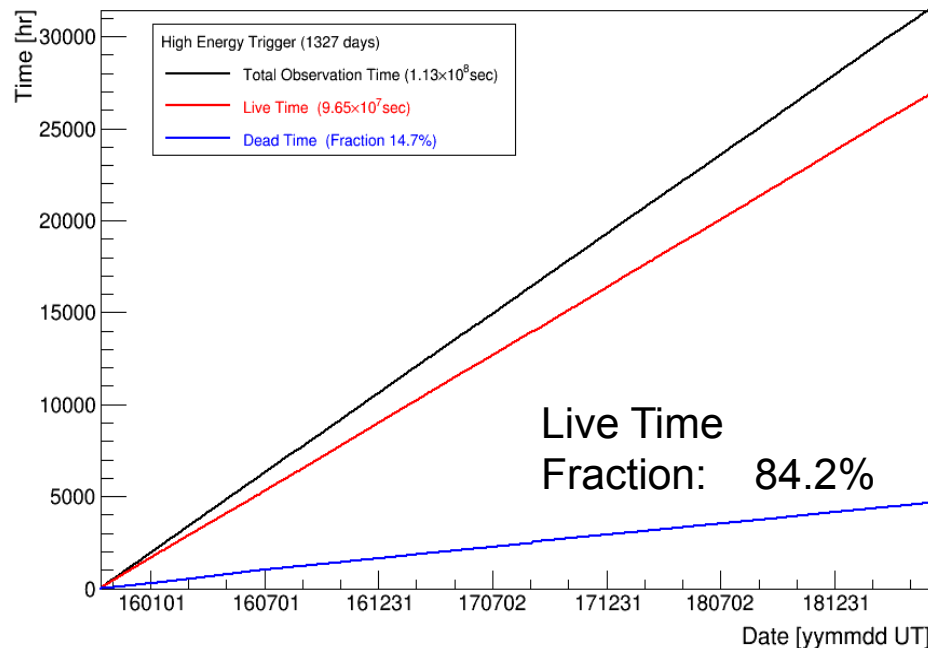


Observations with High Energy Trigger (>10GeV)

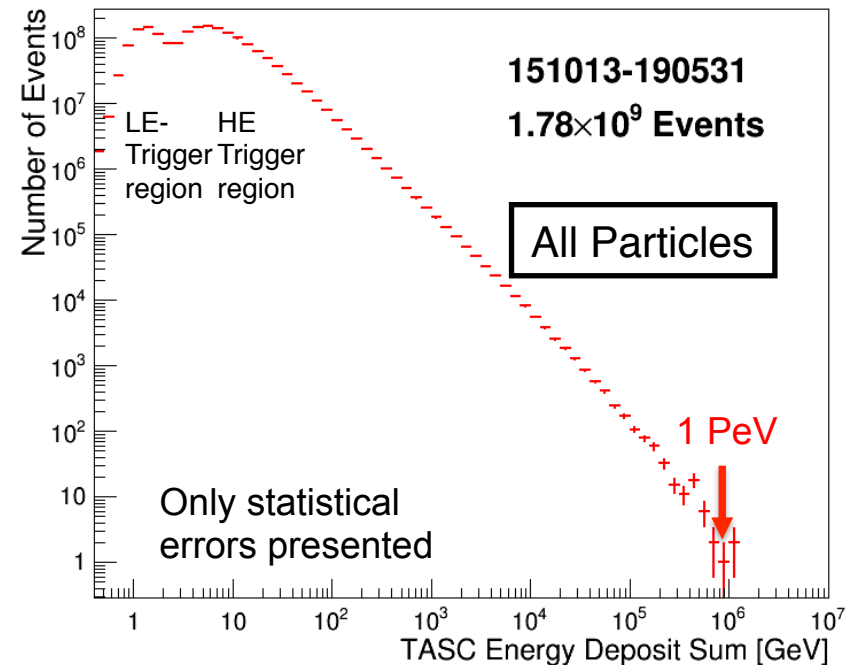
Observation with High Energy Trigger for 1327 days : Oct.13, 2015 – May 31, 2019

- The exposure, SQT , has reached $\sim 116 \text{ m}^2 \text{ sr day}$ for electron observations under continuous and stable operations.
- Total number of triggered events is $\sim 1.8 \text{ billion}$ with a live time fraction of $\sim 84 \%$.

Accumulated observation time (live, dead)



Distribution of deposit energies (ΔE) in TASC



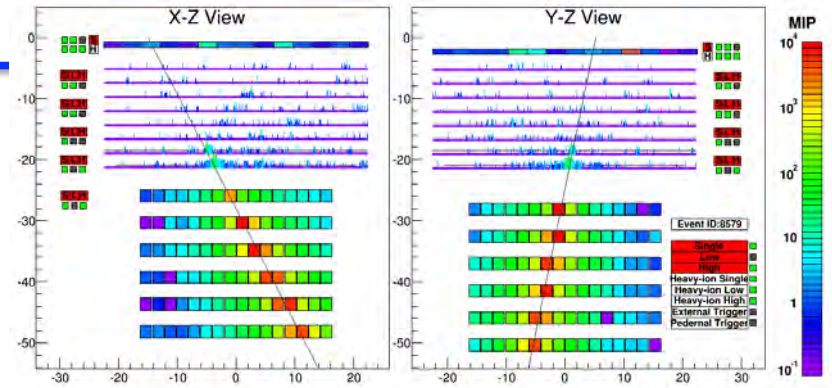


Examples of Observed Events

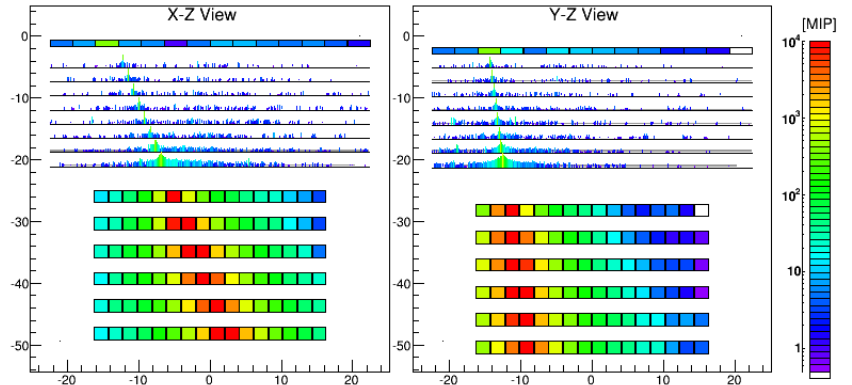
Event Display: Electron Candidate (>100 GeV)



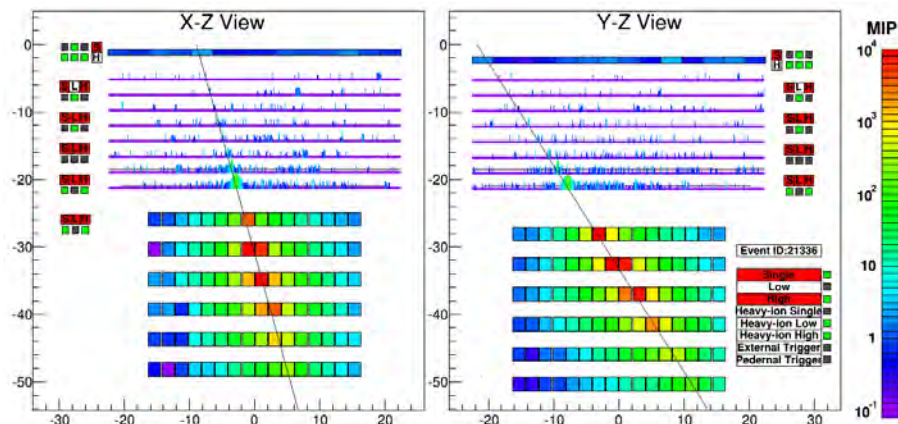
Proton, $\Delta E=2.89$ TeV



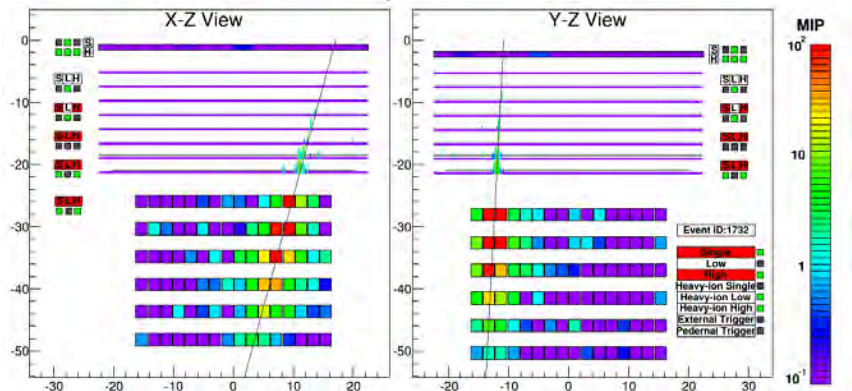
Fe, $\Delta E=9.3$ TeV



Electron, E=3.05 TeV



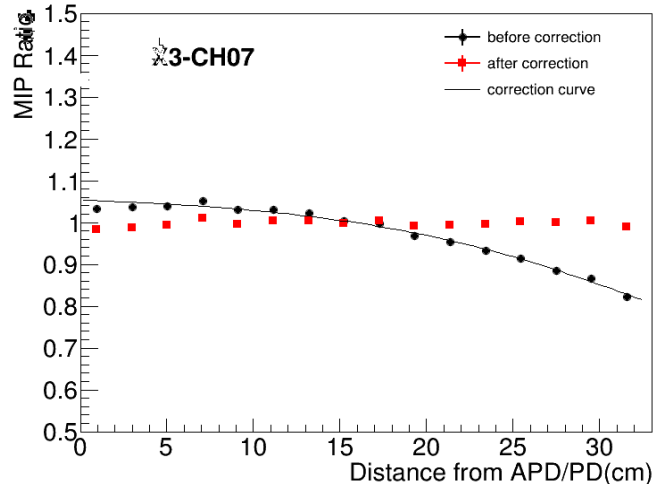
Gamma-ray, E=44.3 GeV



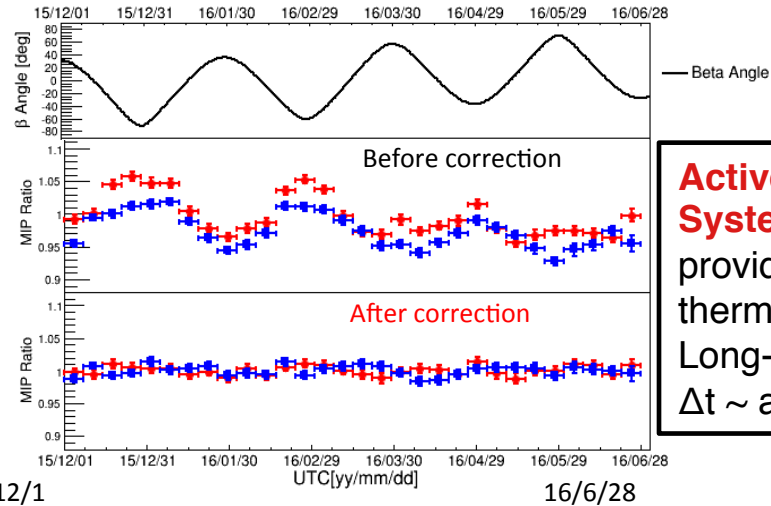


Position and Temperature Calibration + Long-term Stability

Example of **position dependence** correction



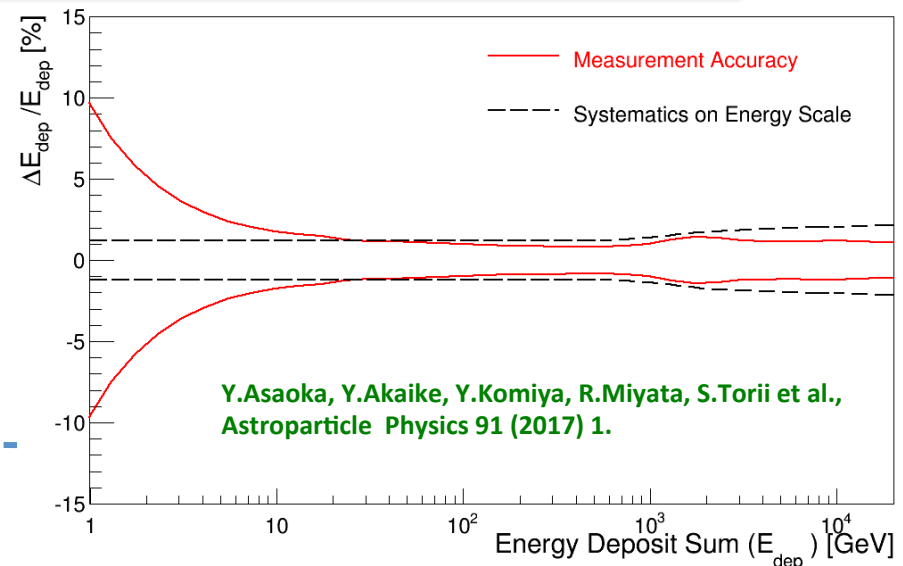
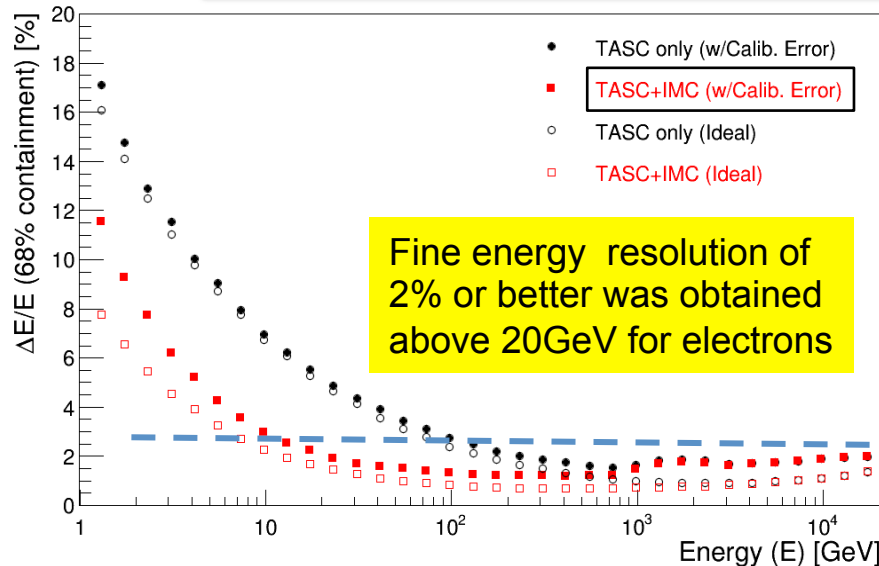
Examples of **temperature change** correction



TASC

Active Thermal Control System (ATCS) on ISS provides very stable thermal condition during Long-term observations: $\Delta t \sim$ a few degrees

Energy Resolution for Electrons by On-orbit Calibration





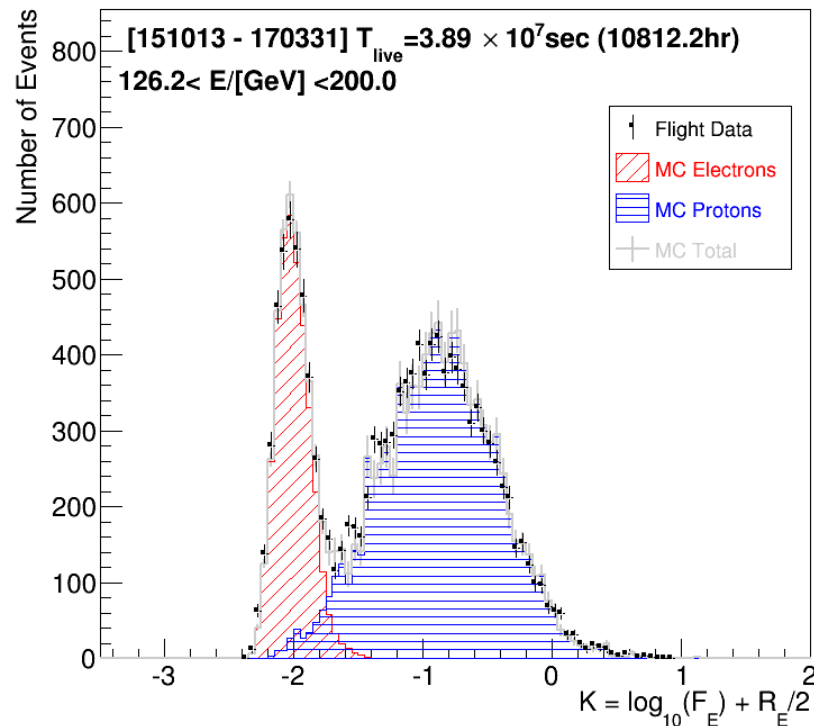
Electron / Proton Discrimination [Y.Asaoka, COSPAR 2018 E1.5-0023-18]

Simple Two Parameter Cut

F_E : Energy fraction of the bottom layer sum to the whole energy deposit sum in TASC
 R_E : Lateral spread of energy deposit in TASC-X1

Cut Parameter K is defined as follows:

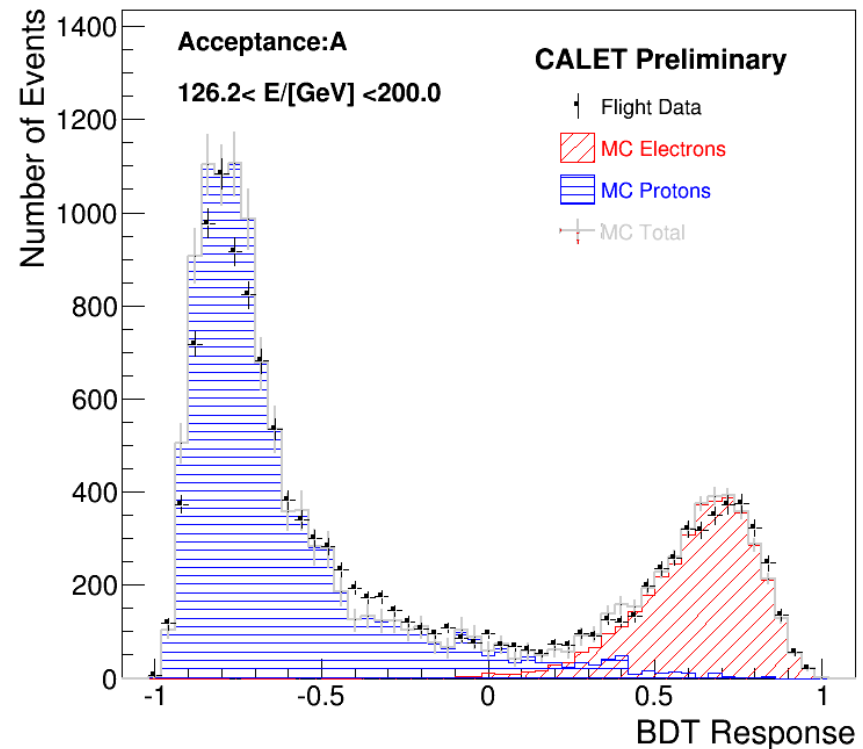
$$K = \log_{10}(F_E) + 0.5 R_E (\text{/cm})$$



Boosted Decision Trees (BDT)

In addition to the two parameters on the left, TASC and IMC shower profile fits are used as discriminating variables

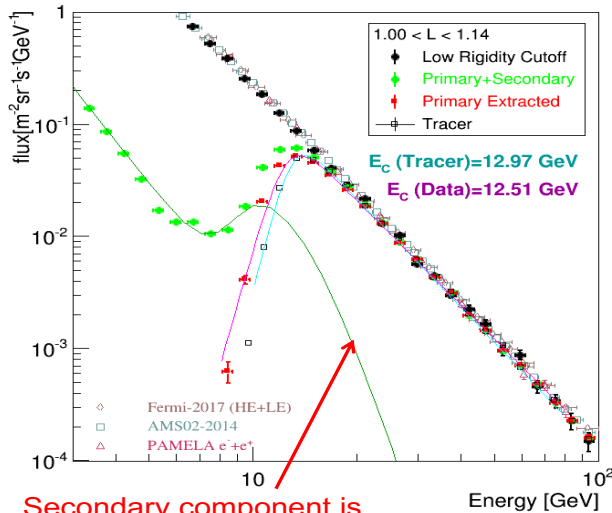
BDT Response using 9 parameters





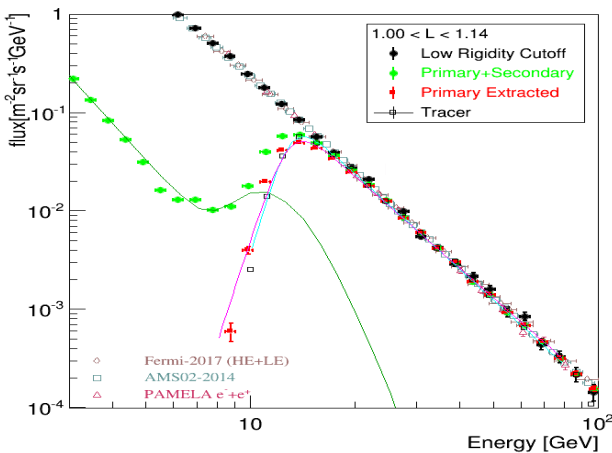
Cutoff Rigidity Measurements and Comparison with Calculation

BEFORE CORRECTION

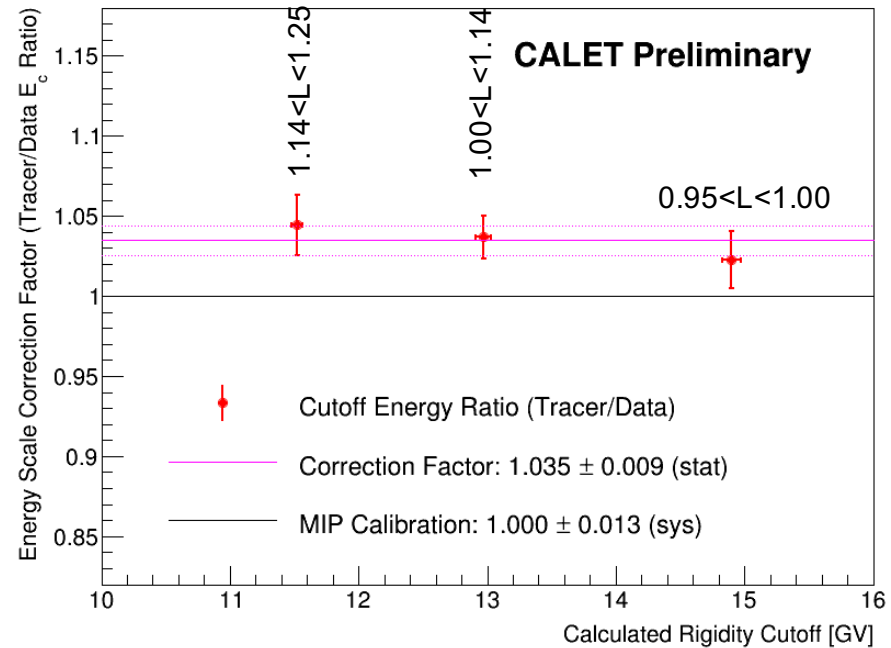


Secondary component is estimated using azimuthal distributions

AFTER CORRECTION



- Performed in three different cutoff rigidity regions.
- Correction factor was found to be **1.035** compared to MIP calibration.



[Y.Asaoka, COSPAR 2018 E1.5-0023-18]

[S.Miyake, COSPAR 2018 E1.5-0027-18]



Systematic Uncertainties in Derivation of Energy Spectrum

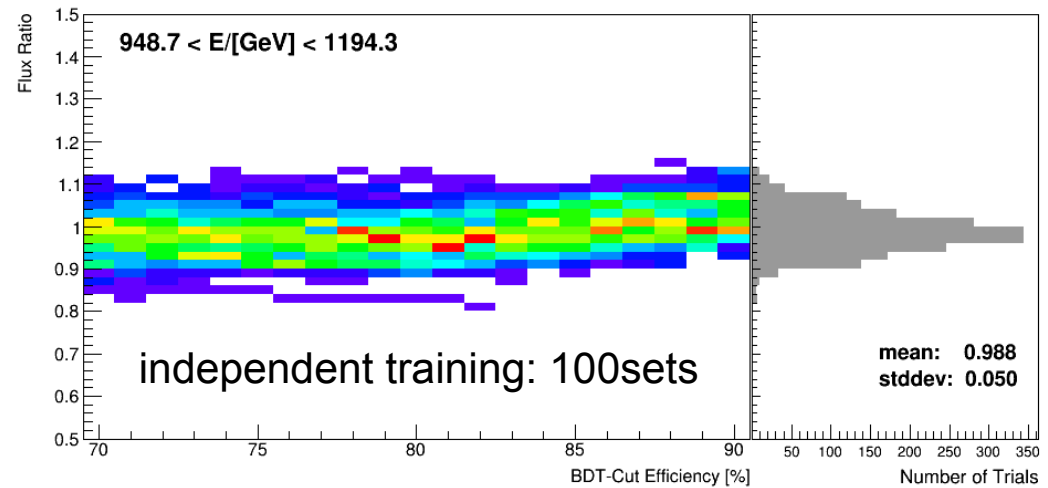
The stability of the measured flux is intensively studied in the large parameter space of analysis selection criteria, including:

- Normalization:
 - Live time
 - Radiation environment
 - Long-term stability
 - Quality cuts
- Energy dependent:
 - Tracking
 - charge ID
 - electron ID (K-Cut vs BDT)
 - BDT stability (vs efficiency & training)
 - MC model (EPICS vs Geant4)

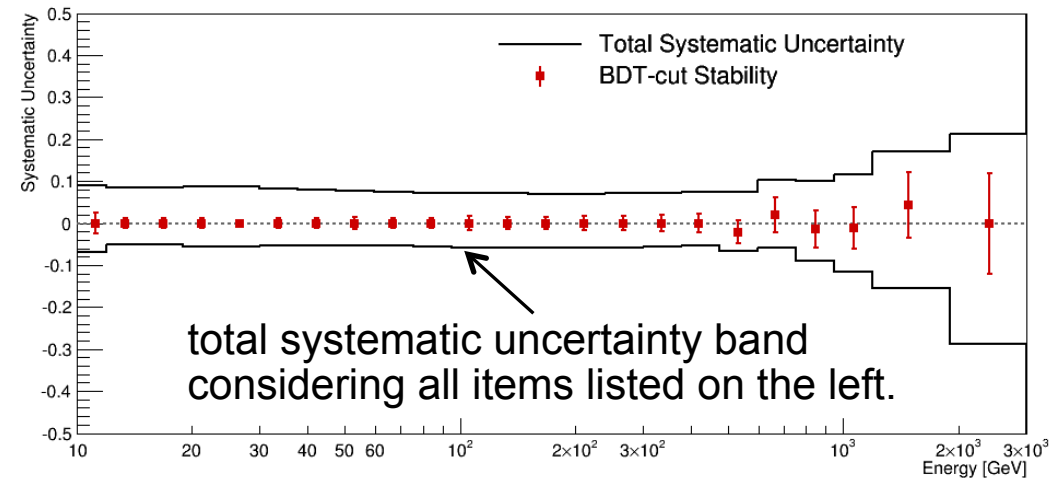
N.B. Energy scale uncertainty is not included in this analysis.

[Y.Asaoka, COSPAR 2018 E1.5-0023-18]

Systematic uncertainty in electron selection by BDT



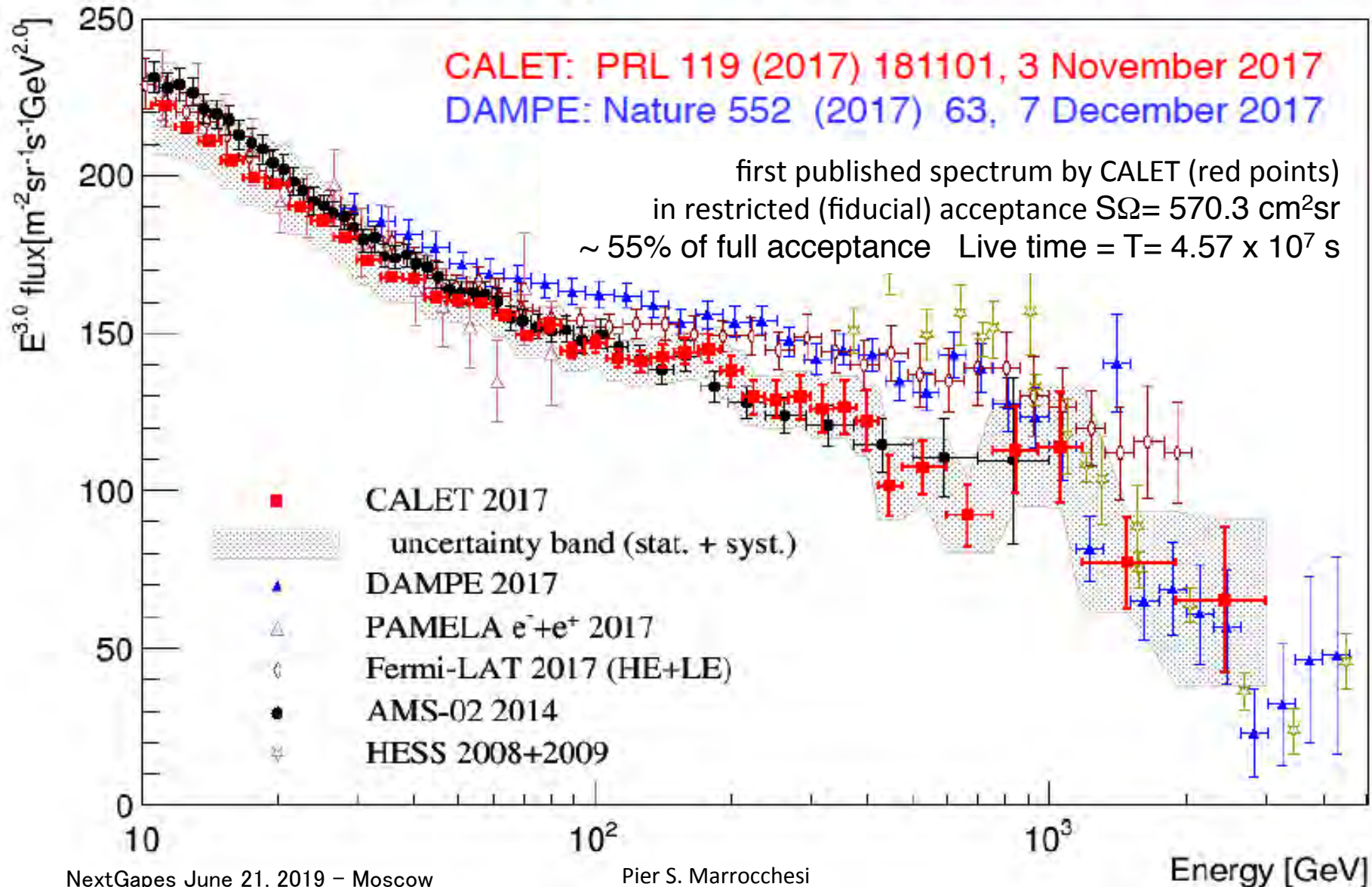
Total systematic uncertainty vs Energy





Direct measurements of the electron spectrum

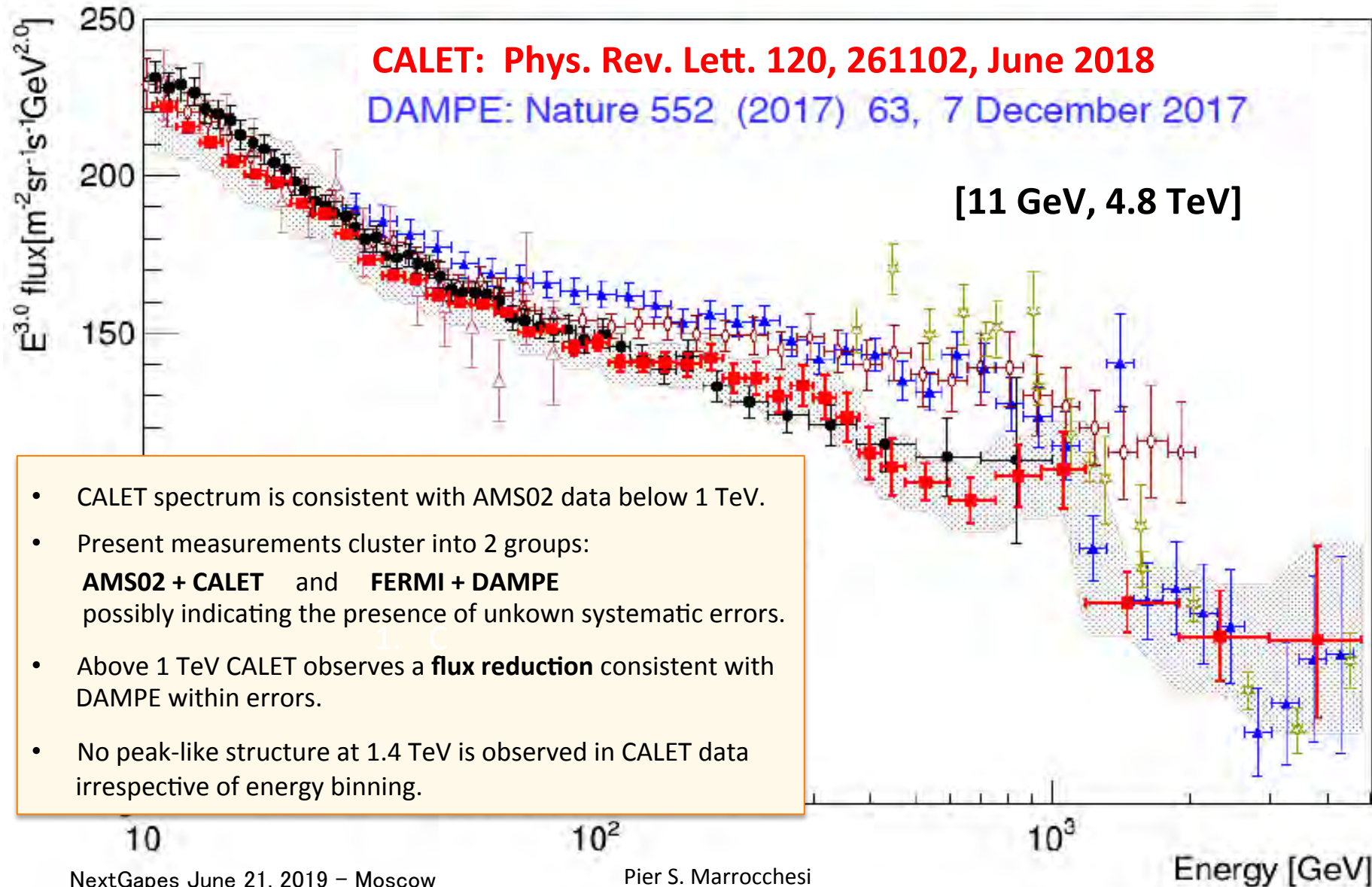
Comparison of CALET with DAMPE and other experiments in space





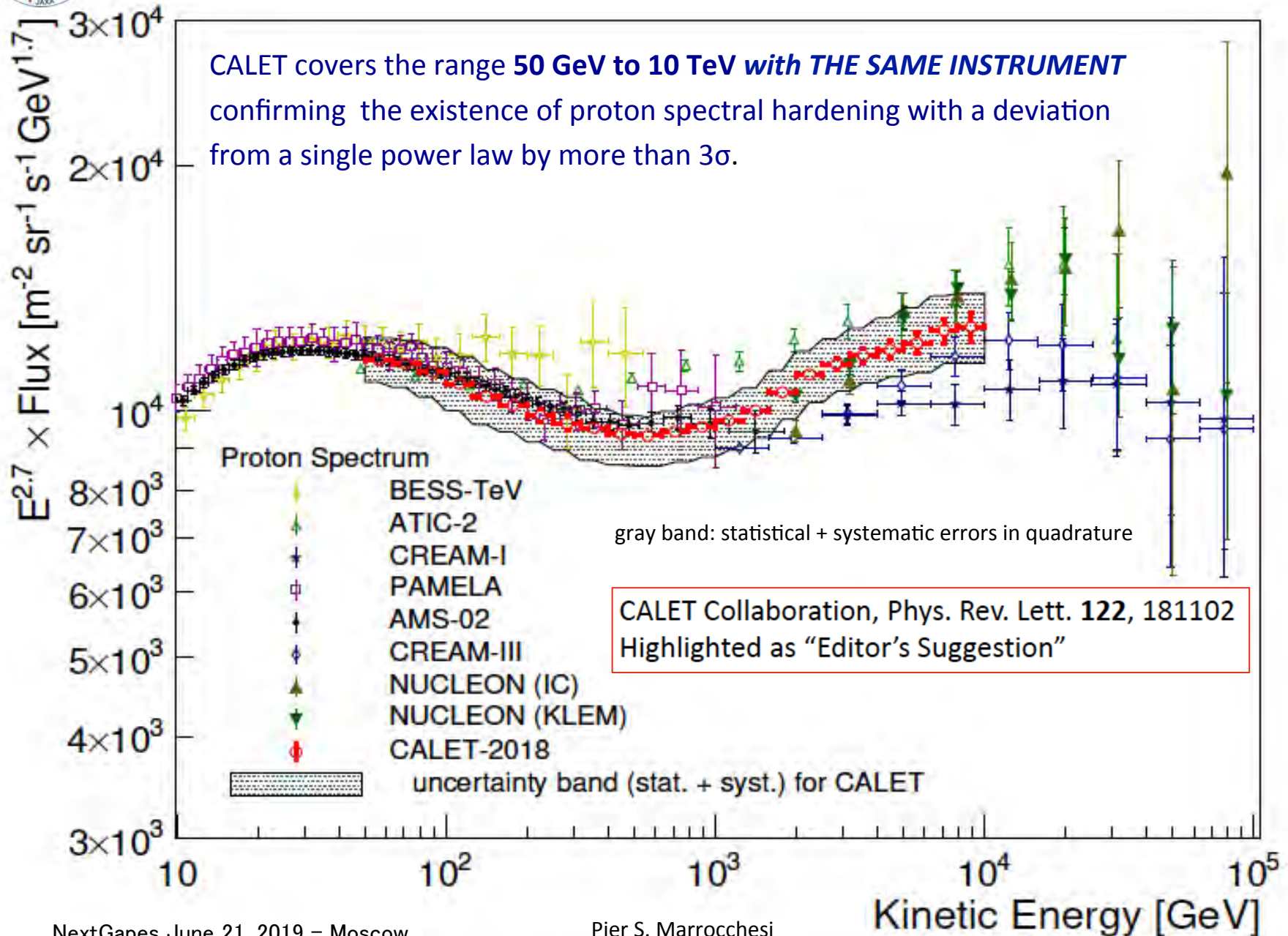
Extended CALET measurement of **electron** spectrum

Approximately doubled statistics above 500GeV by using full acceptance of CALET

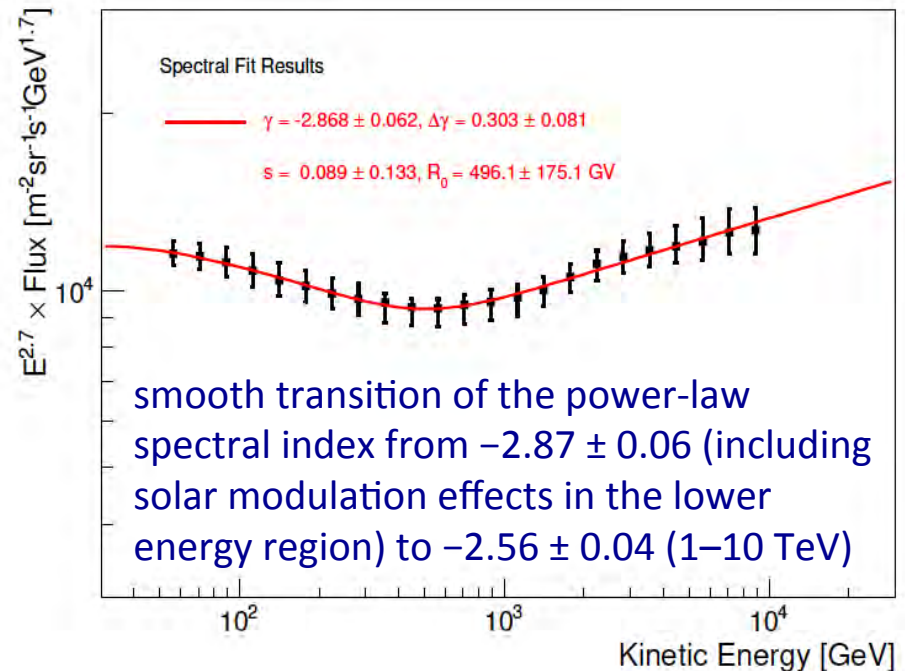
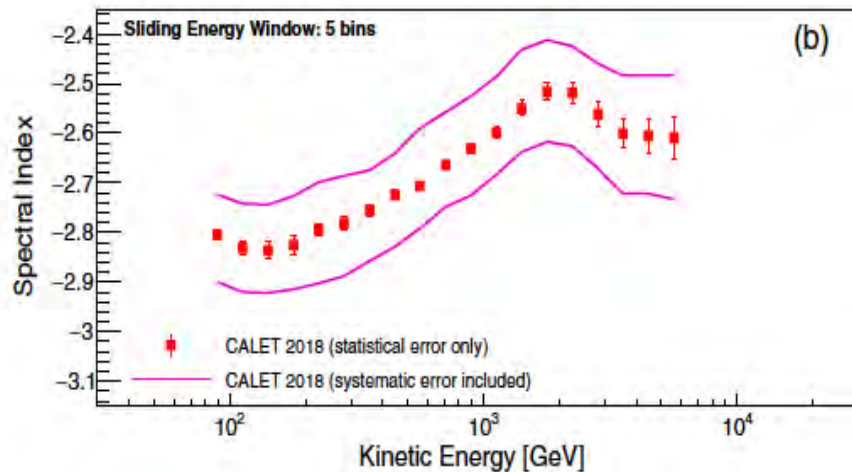
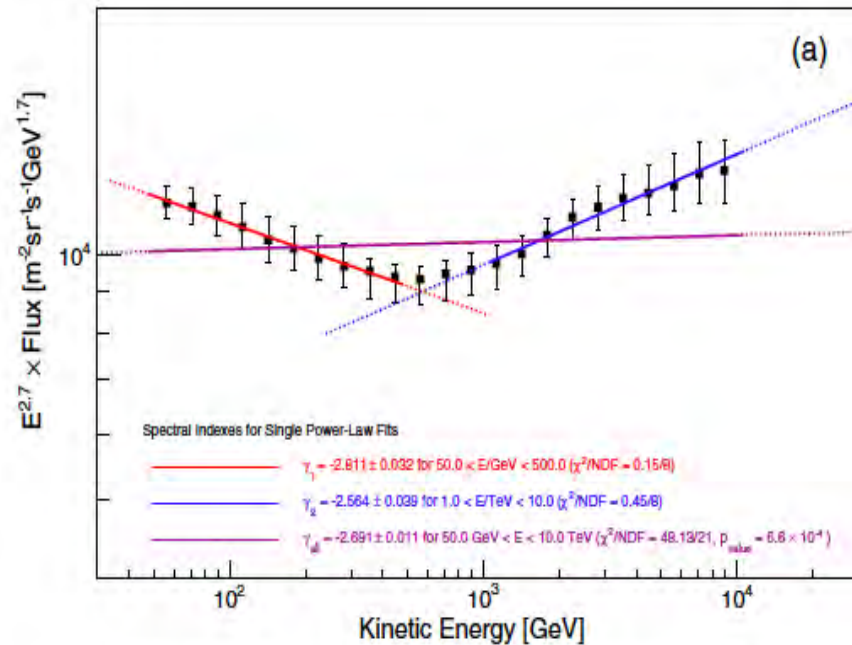




Direct measurement of **proton** spectrum by CALET



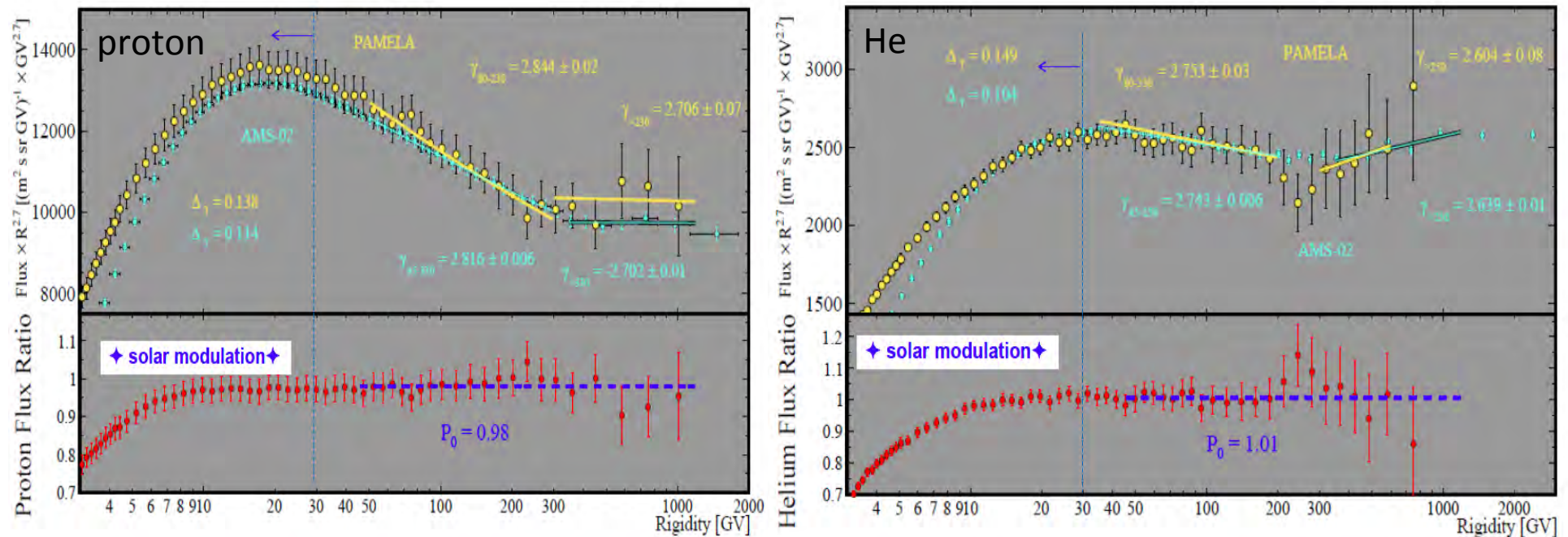
Spectral Behavior of Proton Flux



1. Subranges of 50—500GeV, 1-10TeV can be fitted with single power law function, but not the whole range (significance $> 3\sigma$).
2. Progressive hardening up to the TeV region was observed.
3. “smoothly broken power-law fit” gives power law index consistent with AMS-02 in the low energy region, but shows larger index change and higher break energy than AMS-02.

New era of precision spectral measurements:

- ✧ **p and He below 100 GeV:** % level agreement of magnetic spectrometers (BESS-TeV, PAMELA, AMS02)
- ✧ good agreement of PAMELA and AMS-02 on p and He spectra **below a few hundred GeV**



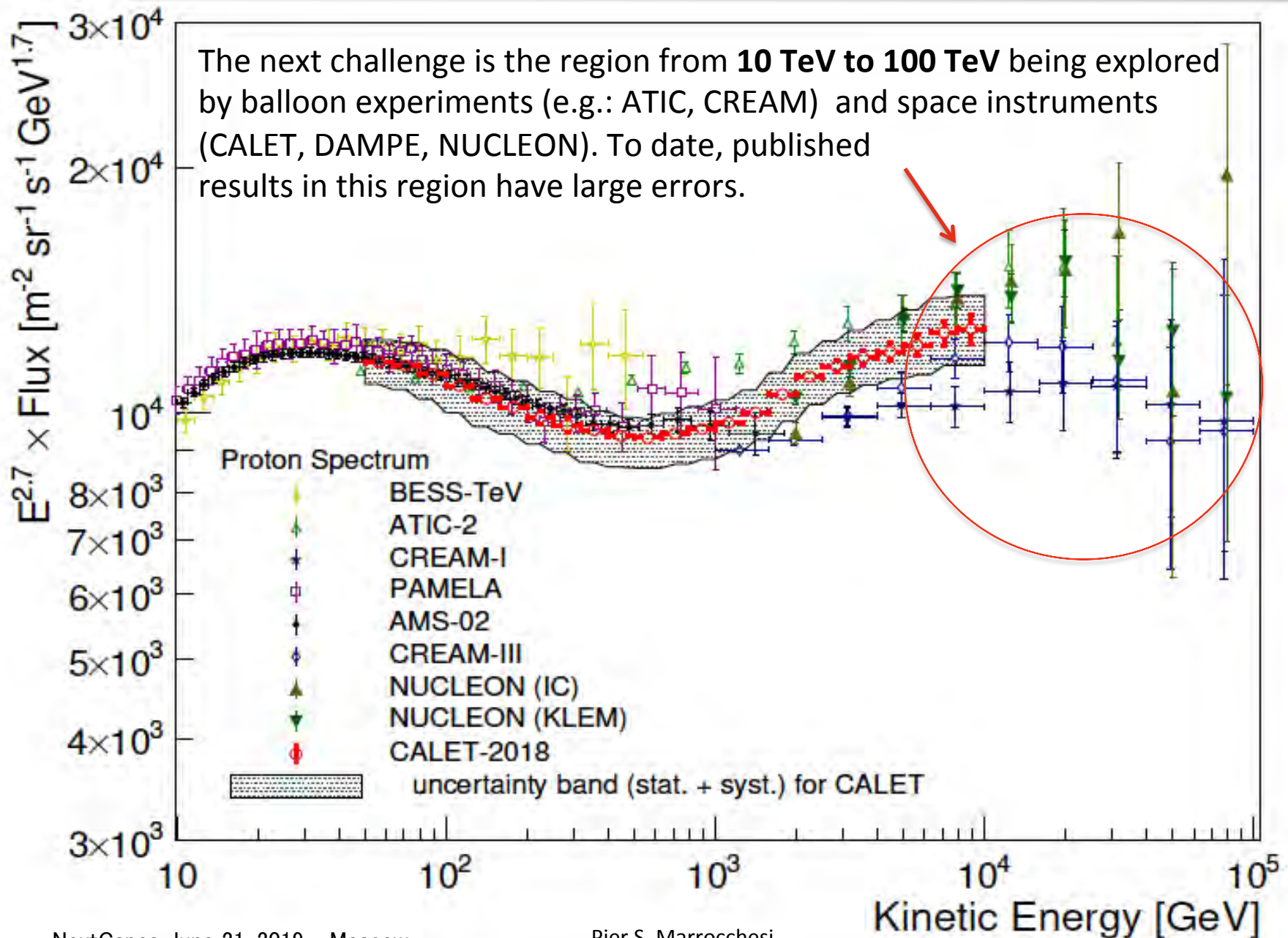
[M.Boezio @LNGS Jul 2016]

O. Adriani et al., Phys. Rep. 544 (2014) 323; M. Aguilar et al., PRL 114 (2015) 171103

O. Adriani et al., Science 332 (2011) 6025; M. Aguilar et al., PRL 115, (2015) 211101

	fit range proton	γ_p	fit range He	γ_{He}
PAMELA	80-230 GV	-2.844 ± 0.02	80-250 GV	-2.753 ± 0.03
AMS-02	45-330 GV	-2.816 ± 0.006	45-250 GV	-2.743 ± 0.006

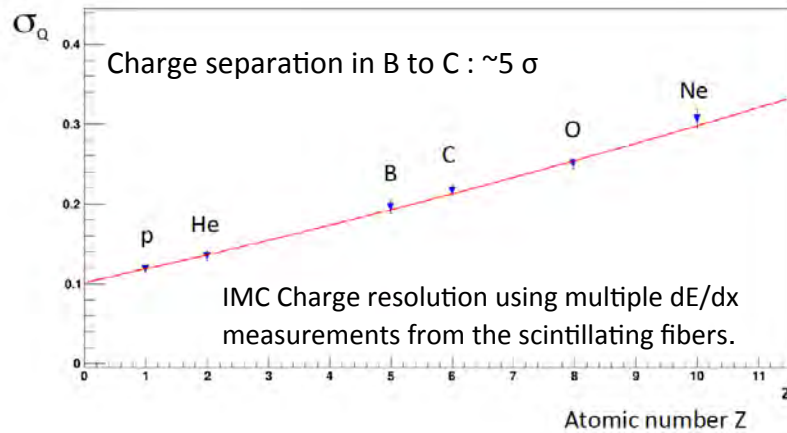
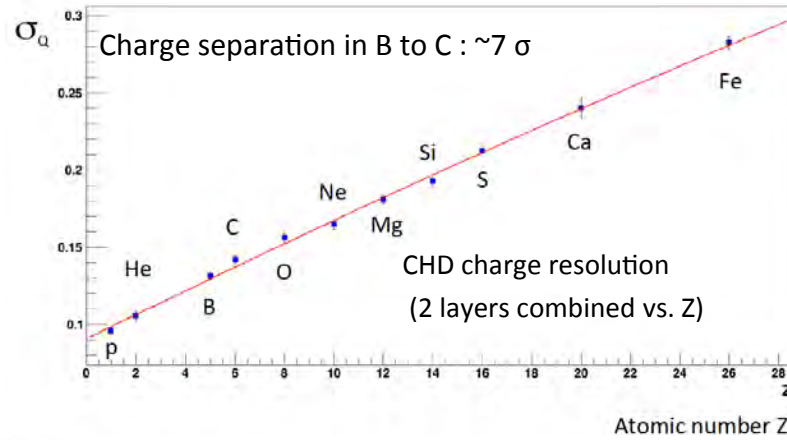
Direct measurements of proton spectrum to date





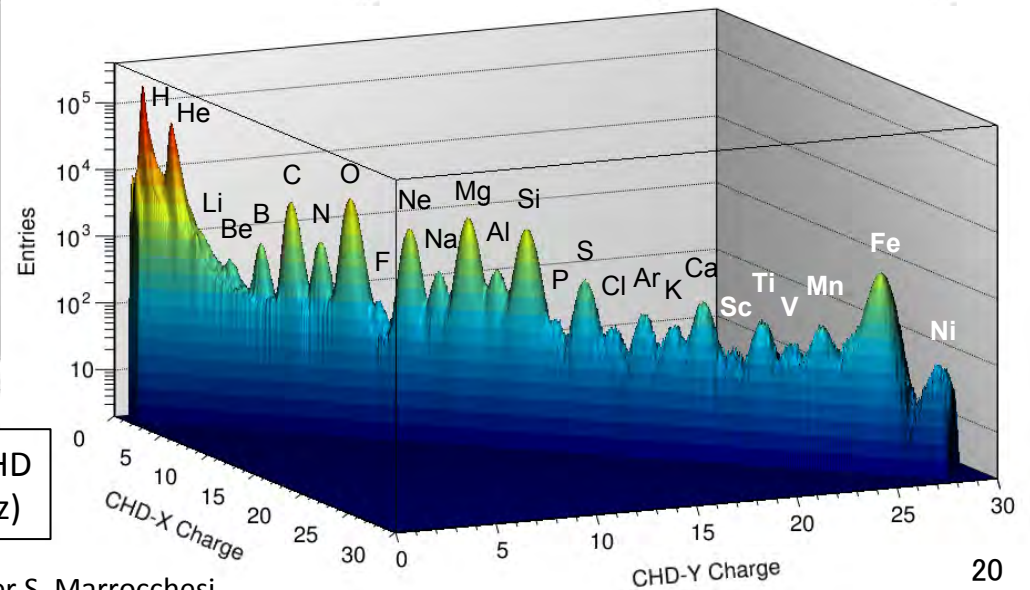
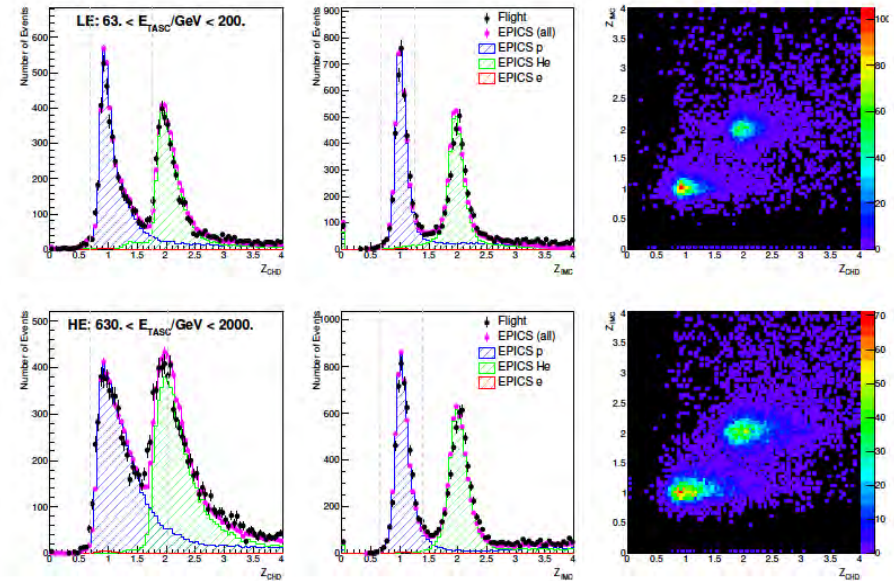
Charge Identification of Nuclei with CHD and IMC

Single element selection for p, He and light nuclei is achieved by CHD+IMC charge analysis.



Deviation from Z^2 response is corrected both in CHD and IMC using a core + halo ionization model (Voltz)

Combined CHD-IMC proton-Helium charge-ID



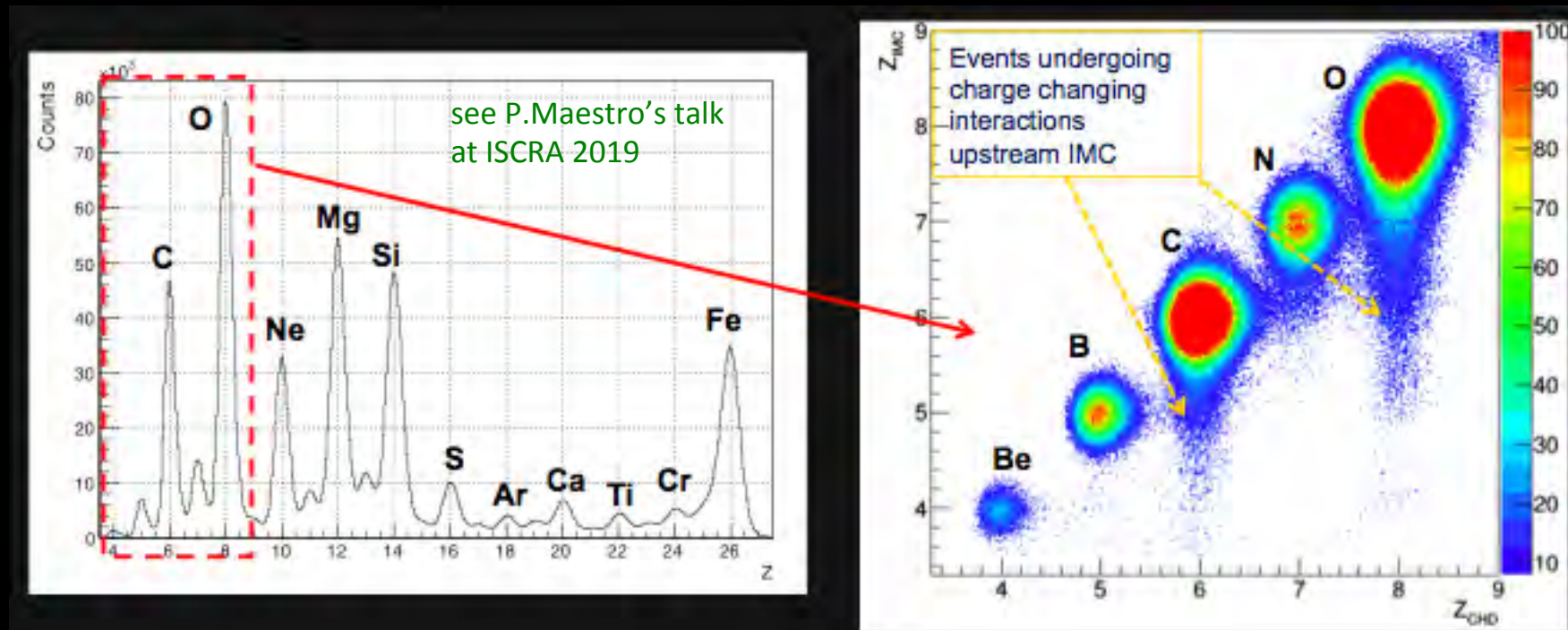


Observation of Light Nuclei

- CALET can identify **individual elements** thanks to the redundant charge determination in CHD and IMC and the excellent charge resolution.

Left: well resolved charge peaks from Be to Fe (all plots are in units of atomic number Z)

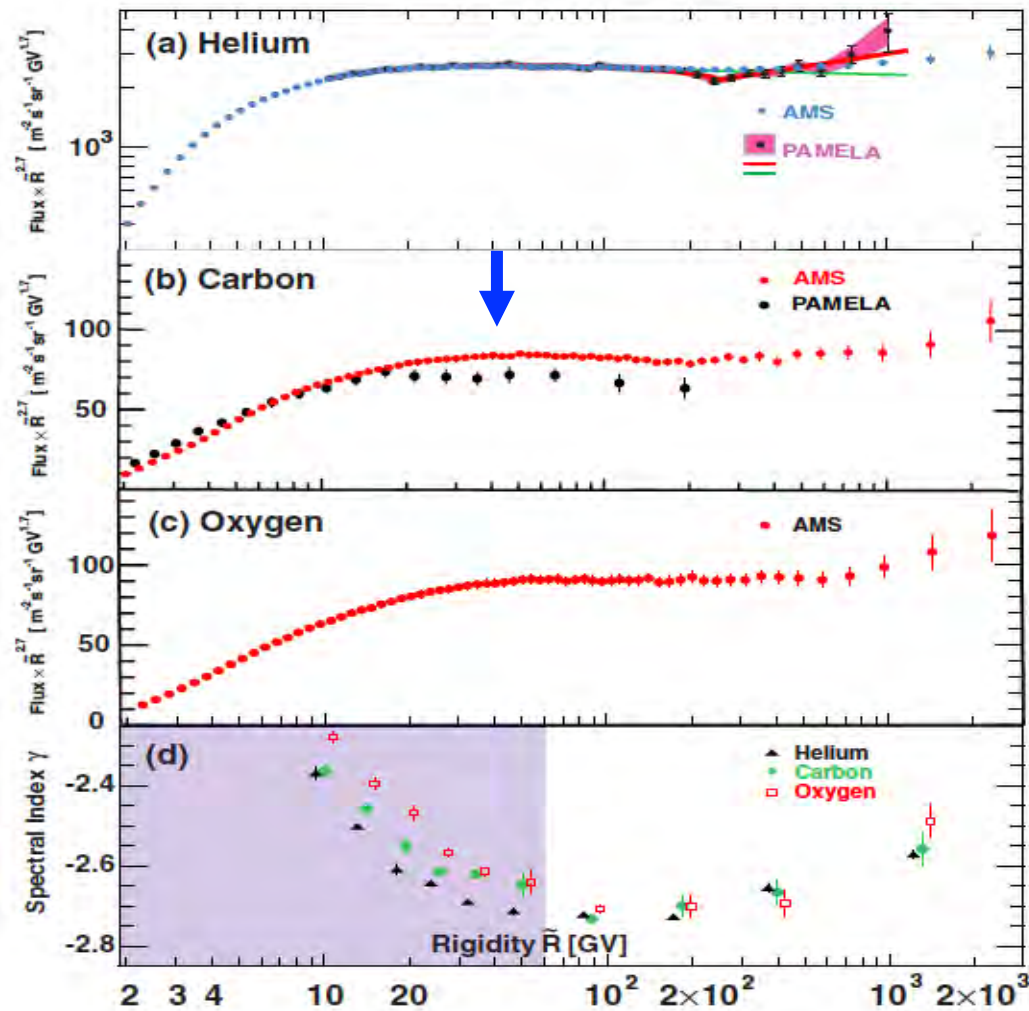
Right: Scatter plot of IMC vs CHD charge



Light Primaries: Carbon and Oxygen

fluxes vs Rigidity from PAMELA and AMS

2018

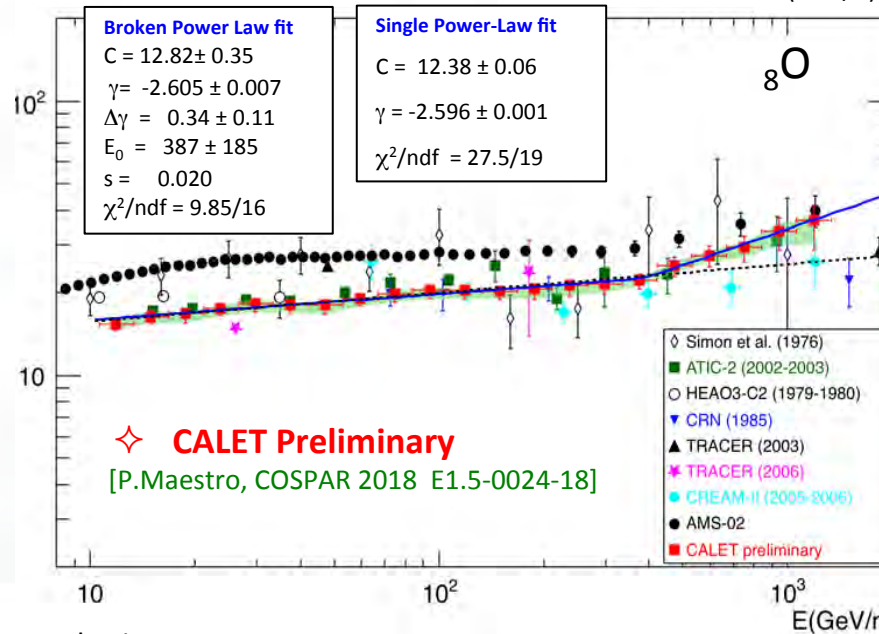
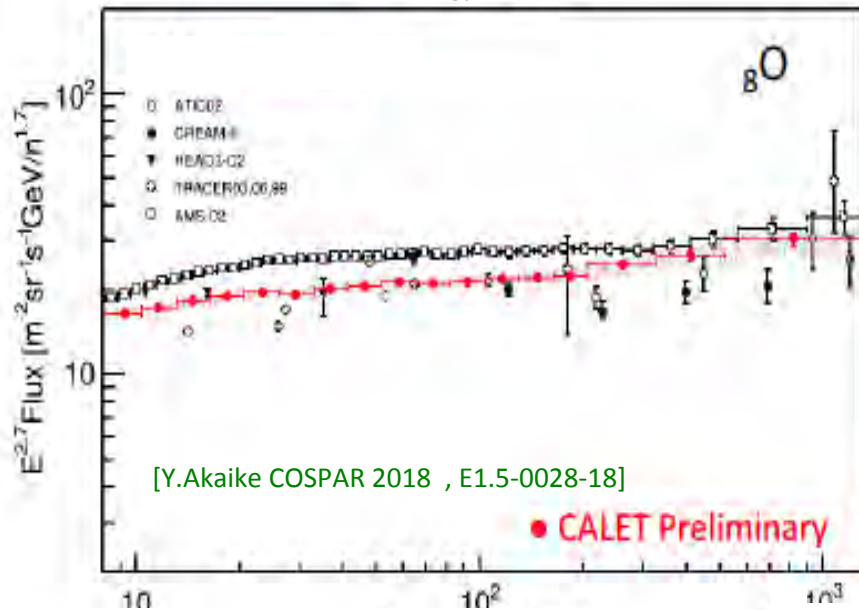
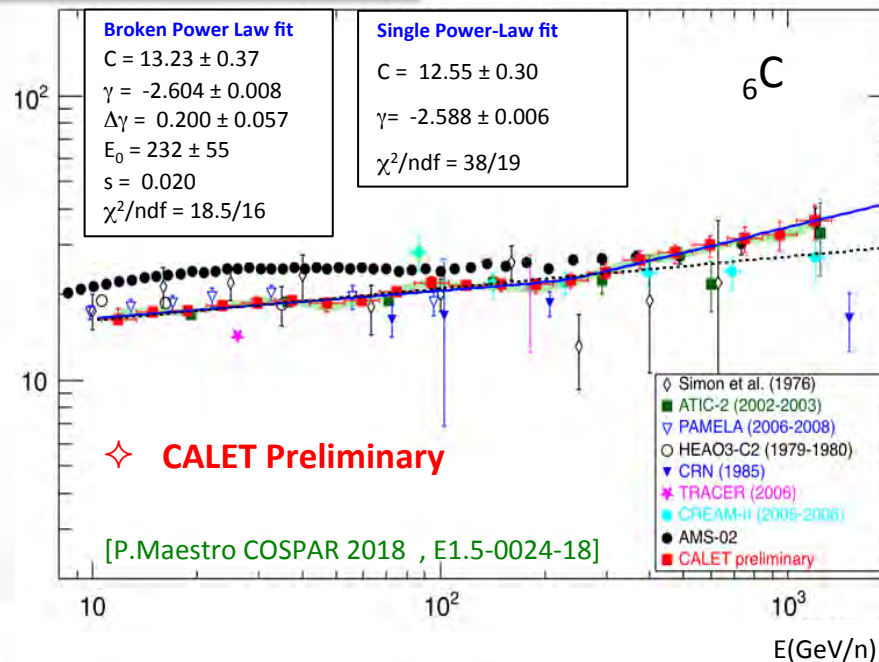
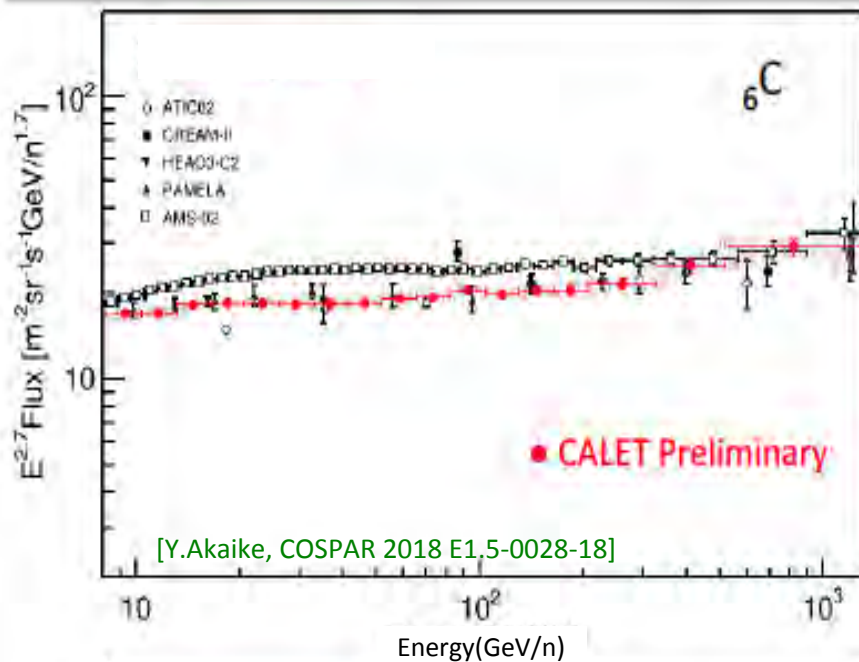


above ~ 10 GV AMS
carbon flux is $\sim 15\%$
higher than PAMELA

no published data
for oxygen flux
by PAMELA

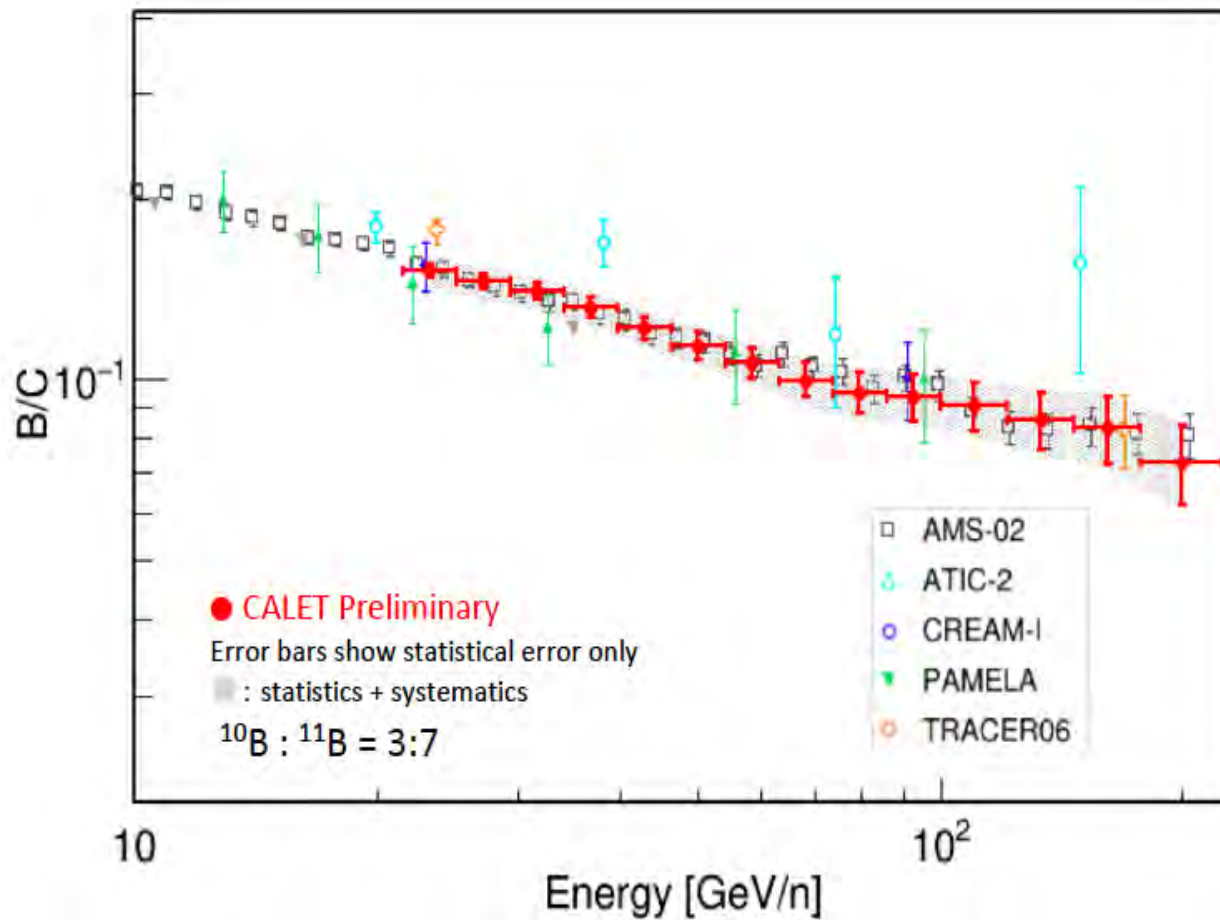
Rigidity (GV)

Preliminary Energy spectra of Carbon and Oxygen (2 independent CALET analyses)





Boron-to-carbon flux ratio (Preliminary)



[Y. Akaike, APS April 14, 2019]

$$^{10}\text{B} : ^{11}\text{B} = 3:7$$

Source of systematic uncertainties

- Trigger efficiency
- Charge consistency cuts
- Track width selection
- Window range for charge identification
- Background model of p and He spectra
- Initial assuming spectra for energy unfolding
- Energy correction base on beam test results
- Difference of beam test model and flight model
- Long term stability



Preliminary Flux of Primary Components

Flux measurements:

$$\Phi(E) = \frac{N(E)}{S\Omega\varepsilon(E)T\Delta E}$$

$N(E)$: Events in unfolded energy bin

$S\Omega$: Geometrical acceptance

$\varepsilon(E)$: Efficiency

T : Live Time

ΔE : Energy bin width

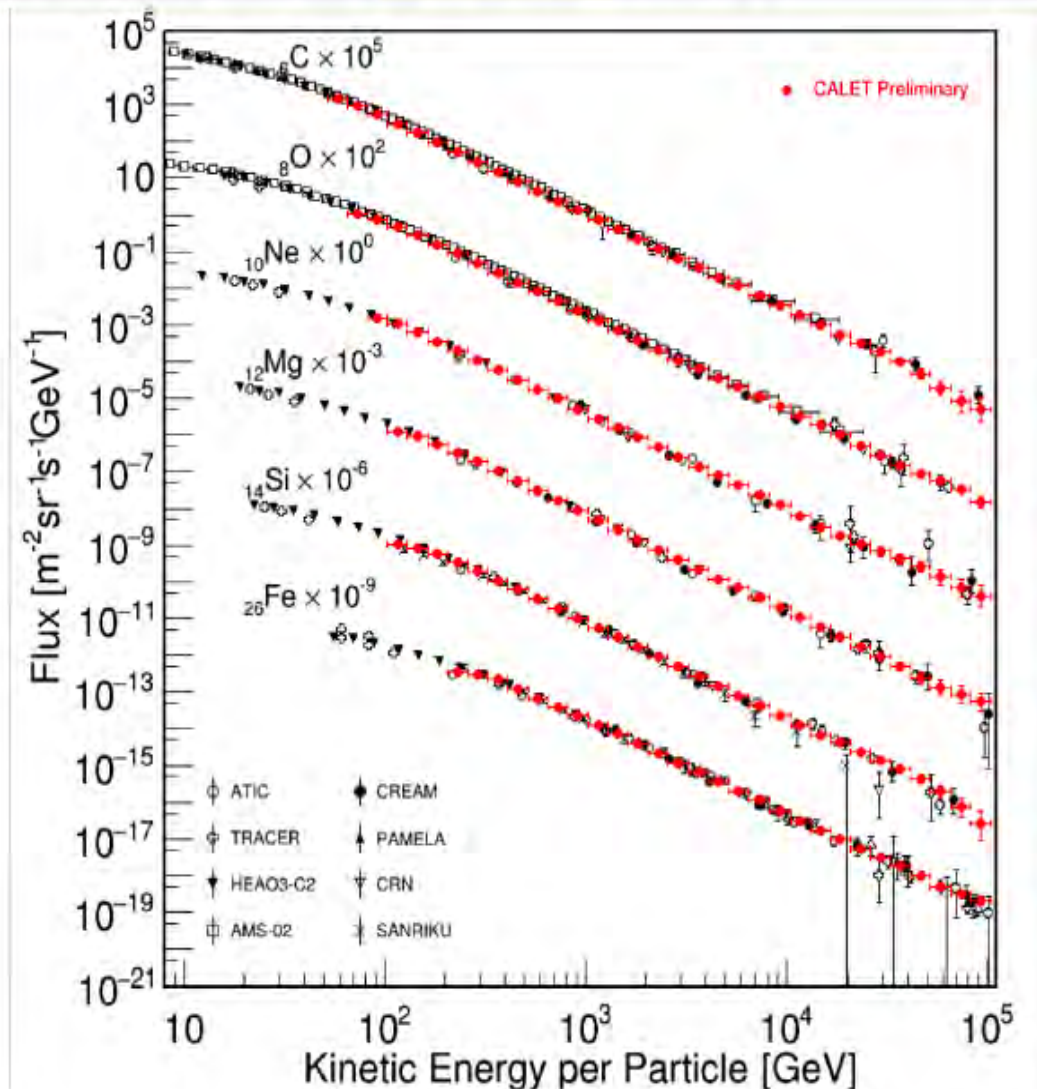
Observation period:

Oct.13 2015 – May.31 2018

(962 days)

5.6×10^6 events (C-Fe, $\Delta E > 10$ GeV)

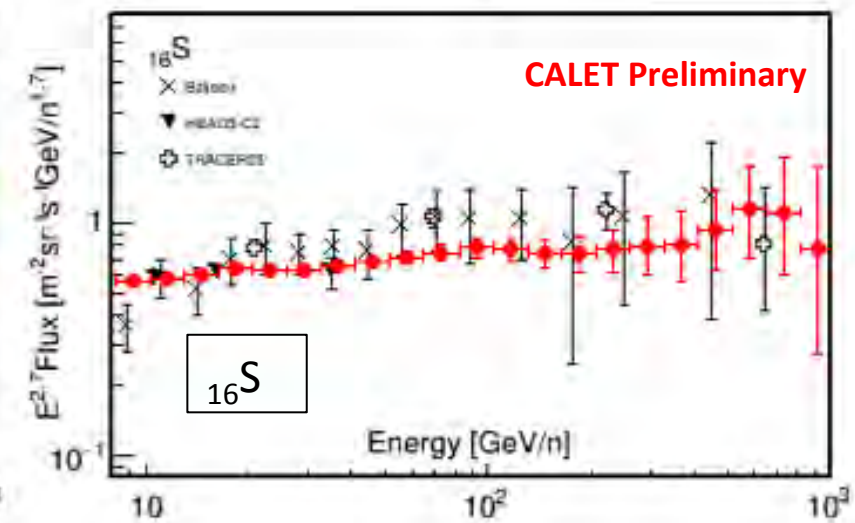
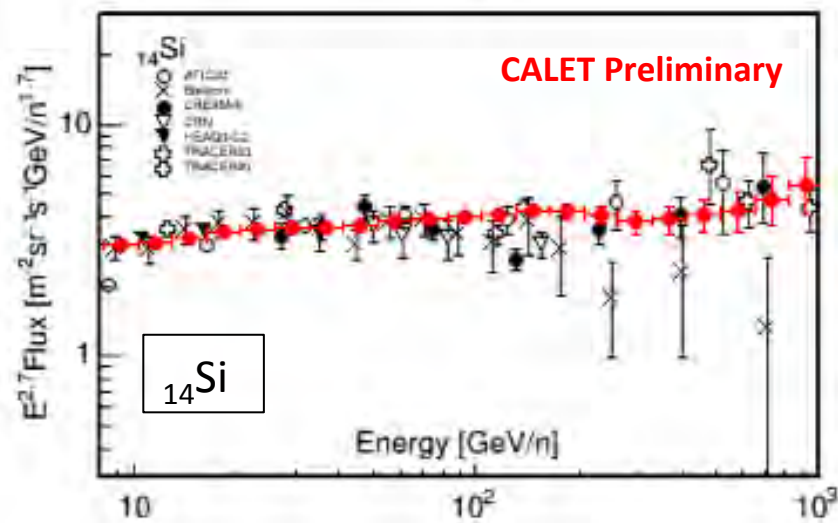
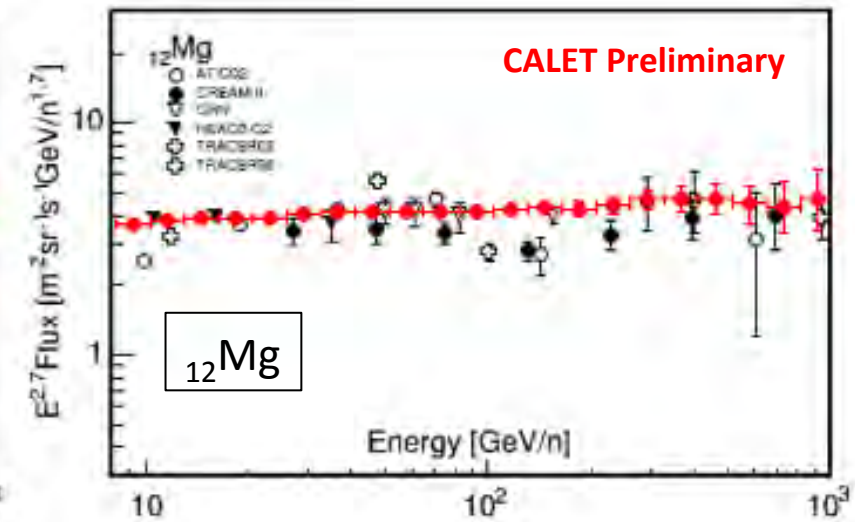
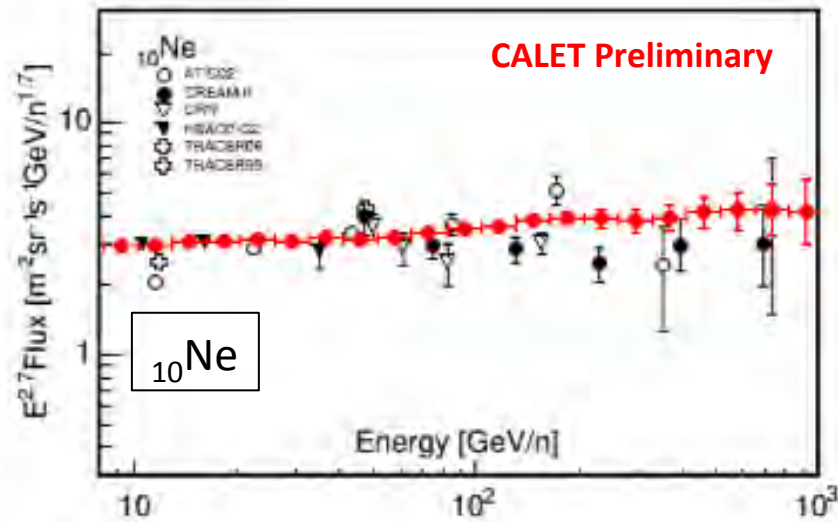
[Y. Akaike, APS April 14, 2019]





Preliminary Spectra of Z-even Nuclei from Ne to S (Z = 10-16)

[Y.Akaike, COSPAR 2018 E1.5-0028-18]

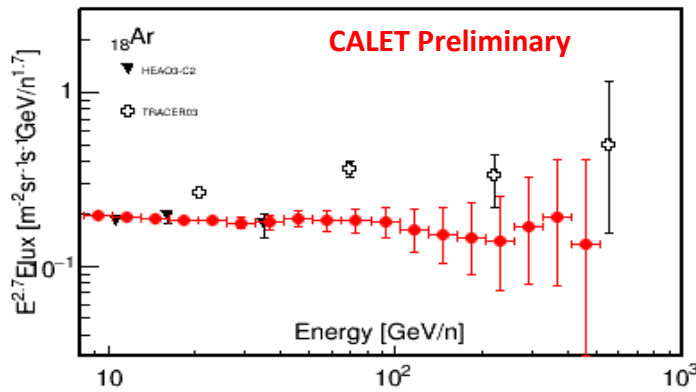




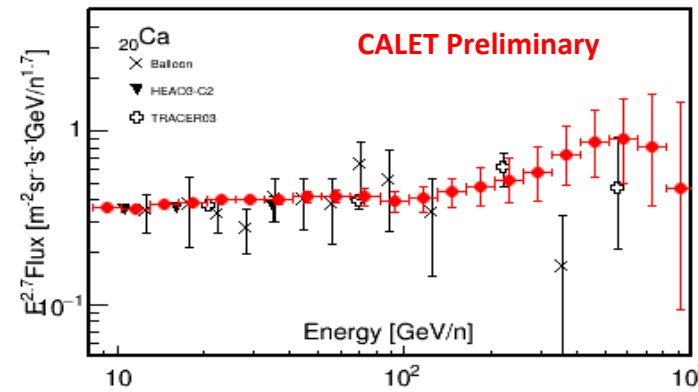
Preliminary Spectra of Z-even Nuclei from Ar to Ni (Z = 18-28)

[Y.Akaike, COSPAR 2018 E1.5-0028-18]

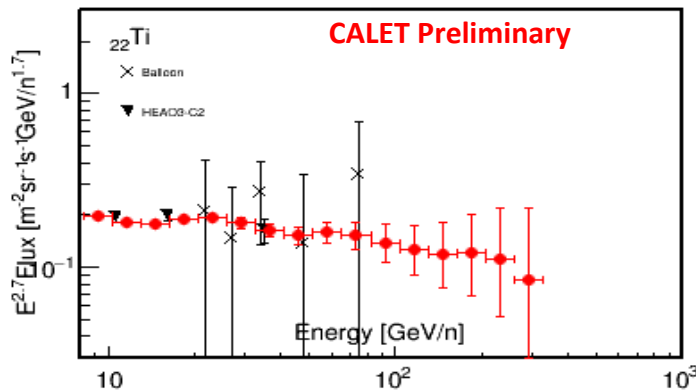
^{18}Ar



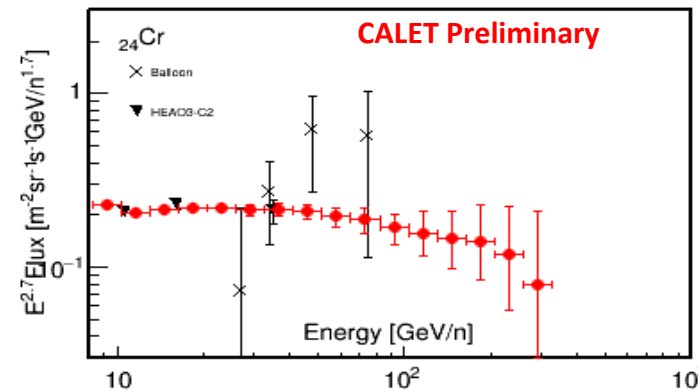
^{20}Ca



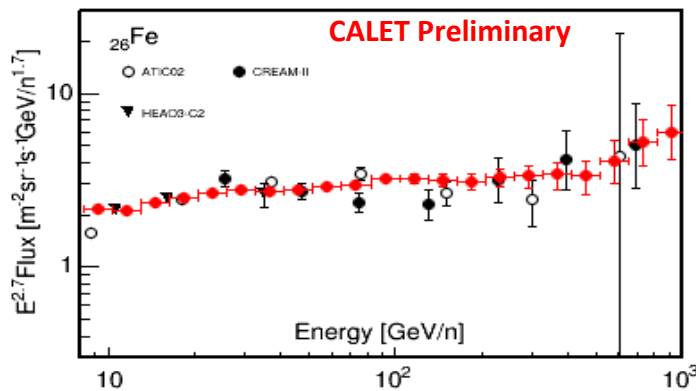
^{22}Ti



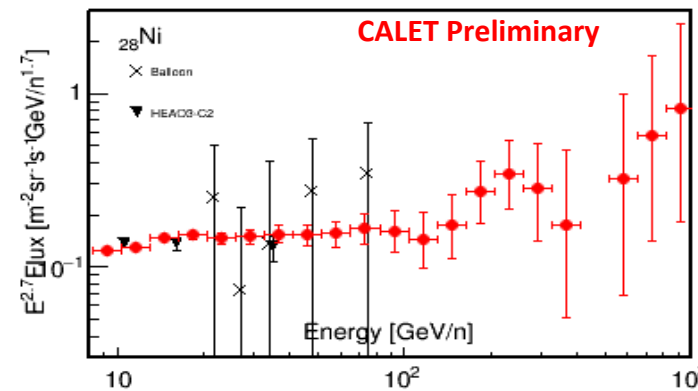
^{24}Cr



^{26}Fe



^{28}Ni





Ultra Heavy Nuclei (Preliminary Measurements for $26 < Z \leq 40$)

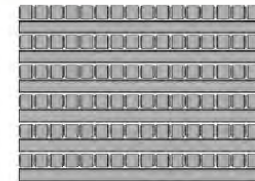
[B.Rauch, APS April 14, 2019]

CALET measures the relative abundances of nuclei above Fe through ${}_{40}\text{Zr}$

CALET has a special UH CR trigger utilizing the CHD and the top 4 layers of the IMC that:

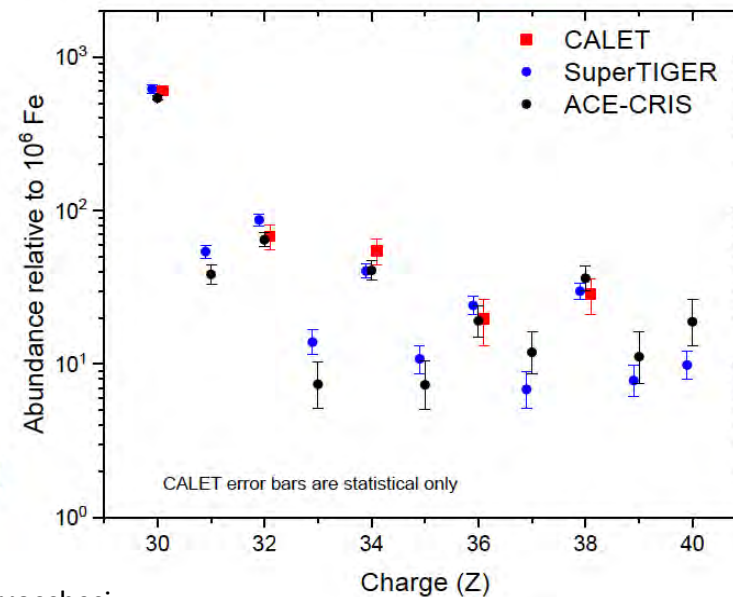
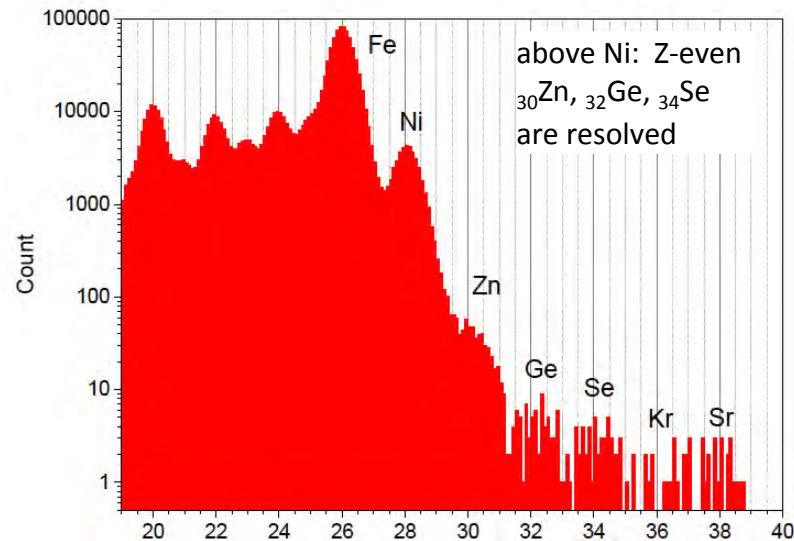
- has an expanded geometry factor of $\sim 4000 \text{ cm}^2\text{sr}$
- has a very high duty cycle due to low event rate

Onboard trigger for UH events



Data analysis

- Event Selection: Vertical cutoff rigidity $> 4\text{GV}$ & Zenith Angle < 60 degrees
- Contamination from neighboring charge are determined by multiple-Gaussian fit
- ◇ The CALET UH element ratios relative to ${}_{26}\text{Fe}$ show good agreement with SuperTIGER and ACE abundances.





CALET γ -ray Sky ($>1\text{ GeV}$)

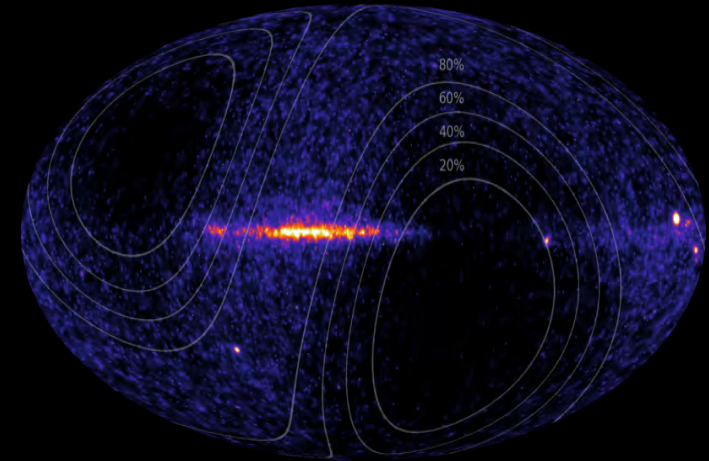
Instrument characterized using EPICS simulations

- Effective area $\sim 400\text{ cm}^2$ above 2 GeV
- Angular resolution $< 2^\circ$ above 1 GeV ($< 0.2^\circ$ above 10 GeV)
- Energy resolution $\sim 12\%$ at 1 GeV ($\sim 5\%$ at 10 GeV)

Simulated IRFs consistent with 2 years of flight data

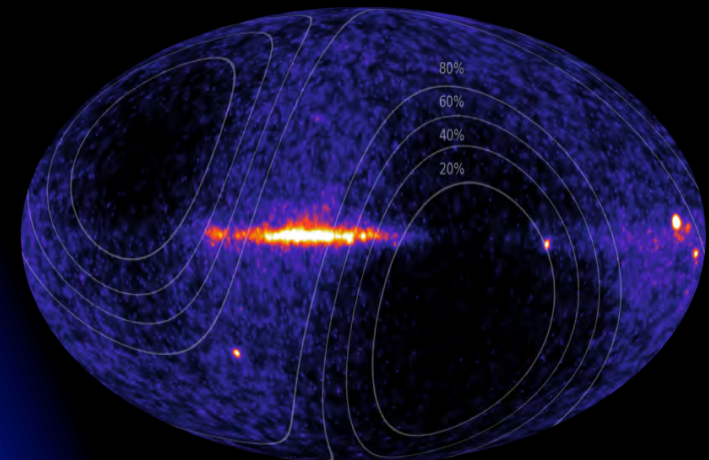
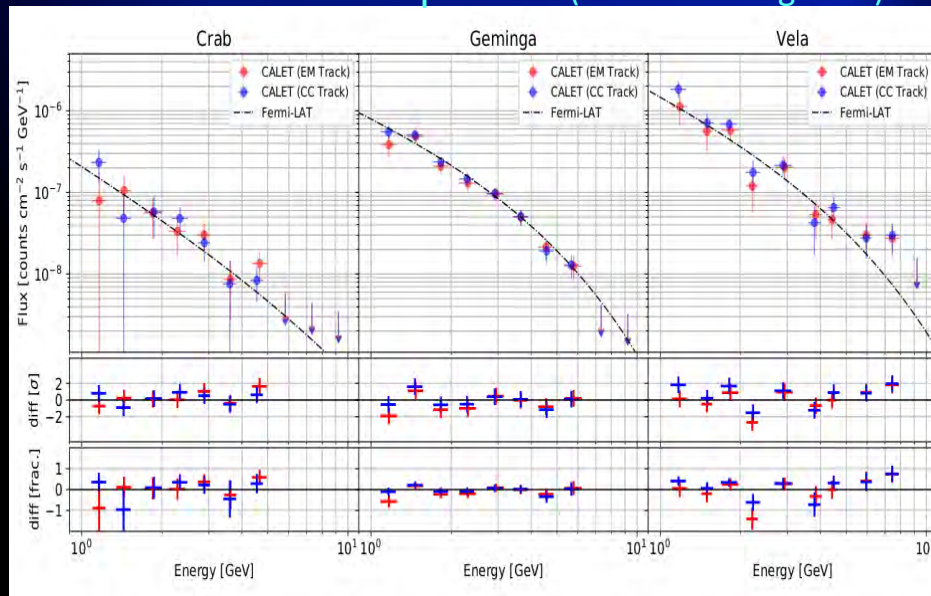
Consistency in signal-dominated regions with Fermi-LAT

Residual background in low-signal regions



[N.Cannady, COSPAR 2018 E1.17-0009-18]

Flux validation with pulsars (under investigation)

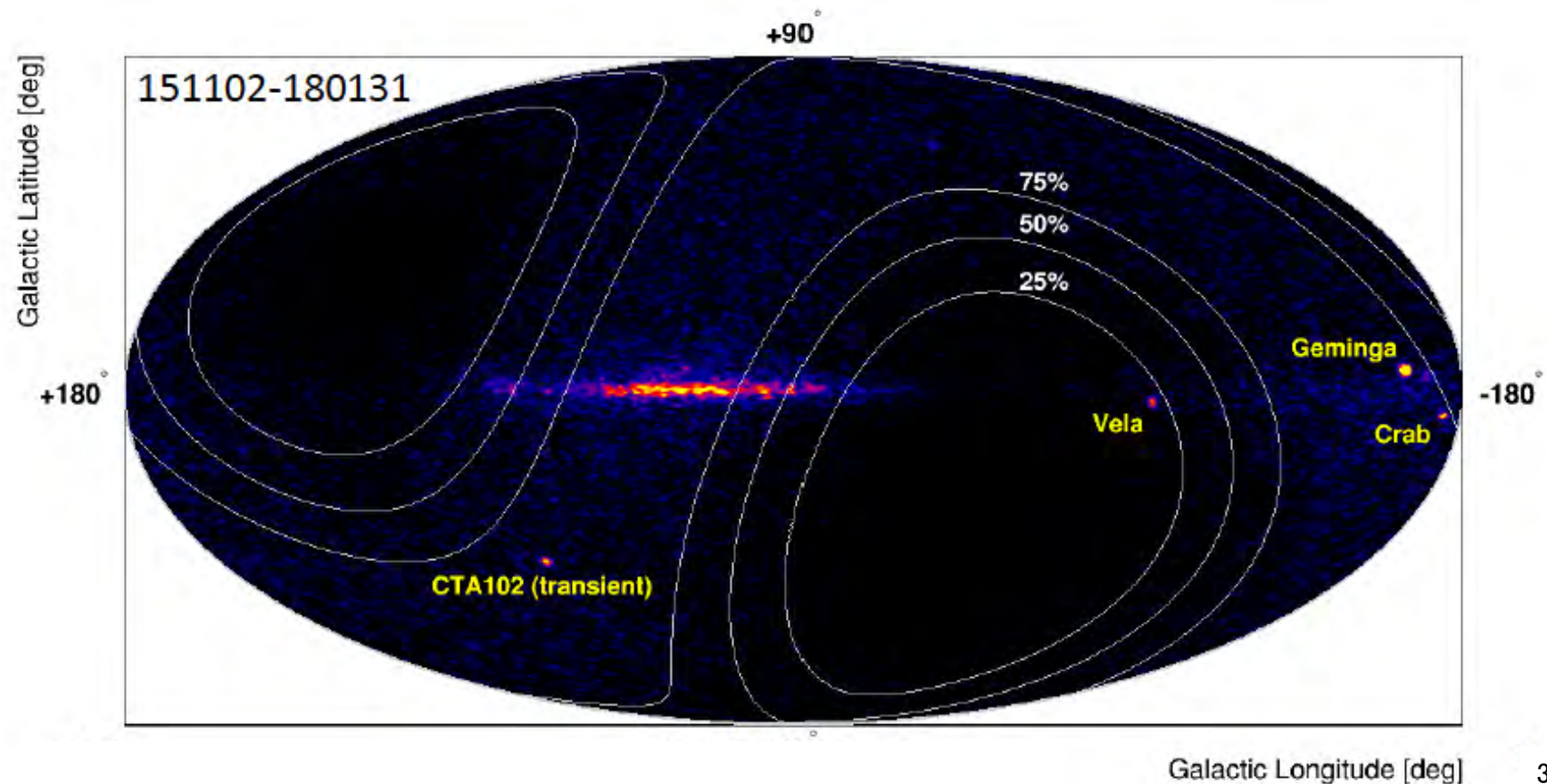
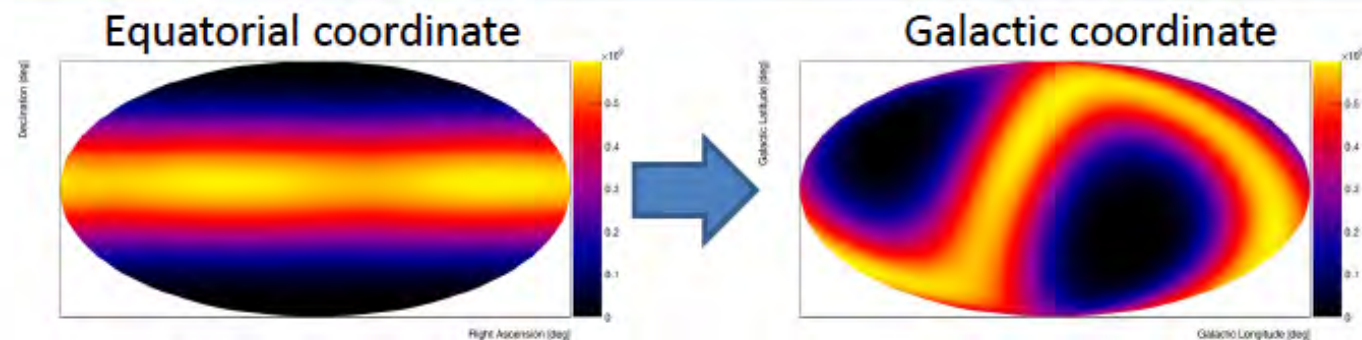


See also: E1.17-0022-18 (Mori & Asaoka)



CALET Sky Map w/ LE- γ Trigger ($E > 1\text{GeV}$)

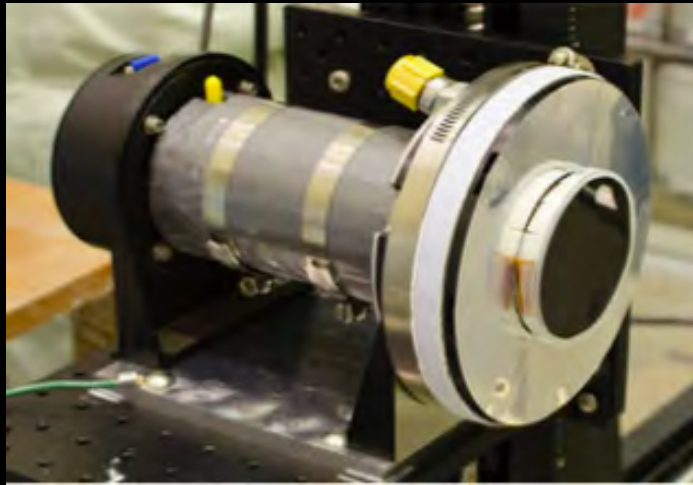
While exposure is not uniform, we have clearly identified the galactic plane and bright GeV sources.





CALET Gamma-ray Burst Monitor (CGBM)

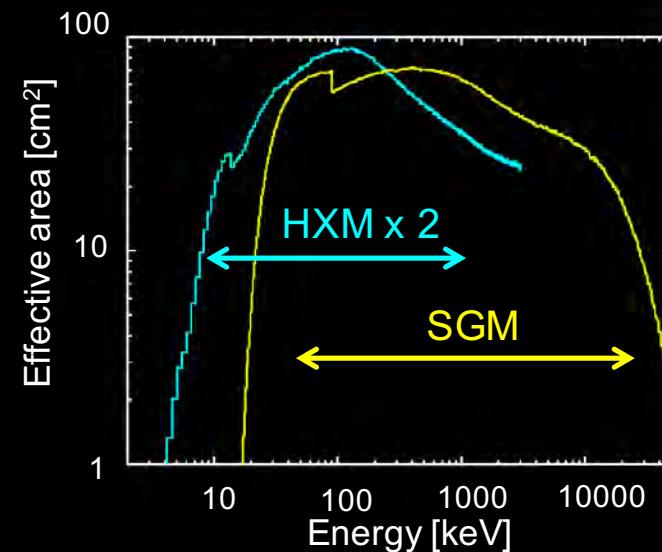
Hard X-ray Monitor (HXM)



Soft Gamma-ray Monitor (SGM)



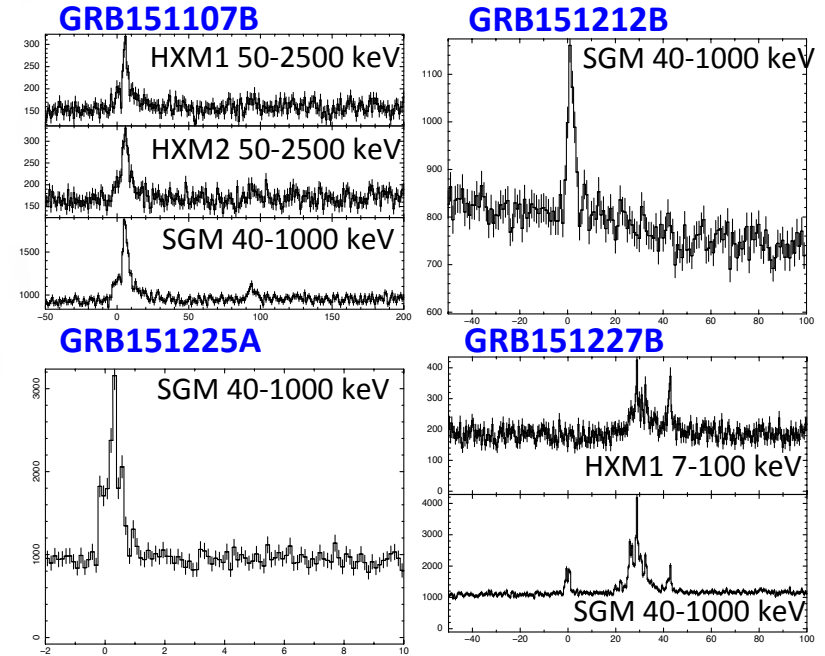
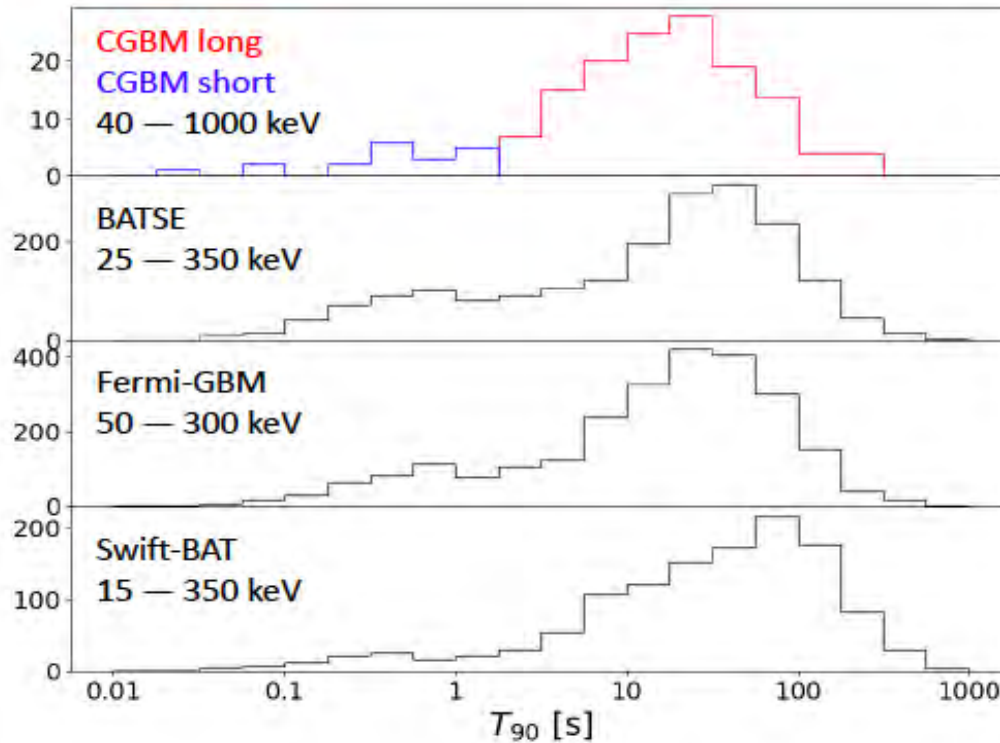
	HXM (x2)	SGM
Detector (Crystal)	LaBr ₃ (Ce)	BGO
Number of detectors	2	1
Diameter [mm]	61	102
Thickness [mm]	12.7	76
Energy range [keV]	7-1000	100-20000
Energy resolution@662 keV	~3%	~15%
Field of view	~3 sr	~2 π sr



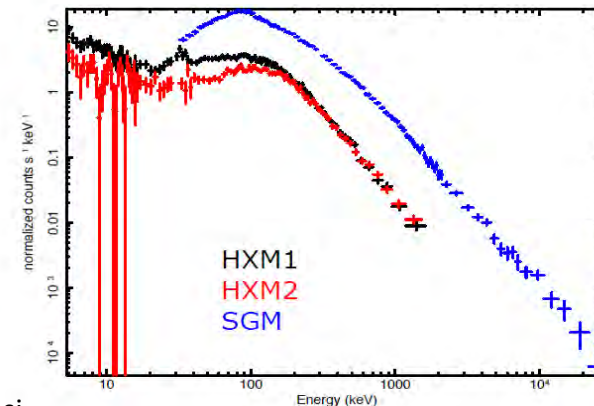


CGBM Observations Summary

Examples of Light Curves



Raw count spectra of GRB 160625B

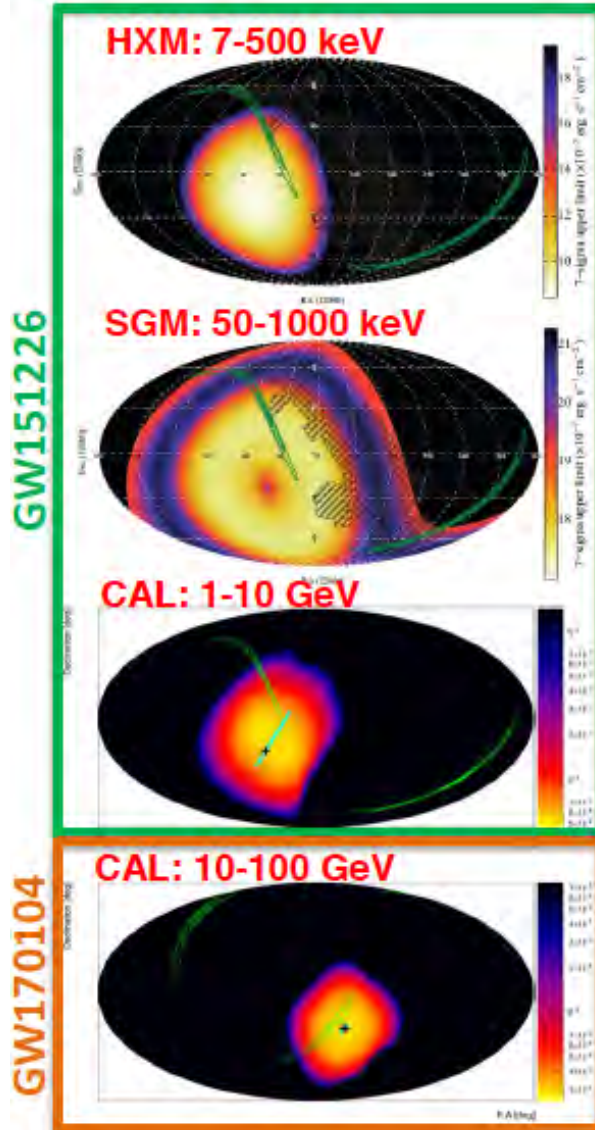


- ✧ As of June 2019:
- 159 GRBs detected**
- 140 Long (88%) 19 Short (12%)**
- Average rate ~ 43 GRBs/year**



Complete Search Results for GW Events during O1&O2

GW151226: O. Adriani et al. (CALET Collaboration), ApJL 829:L20 (2016).
All O1 & O2: O. Adriani et al. (CALET Collaboration), ApJ 863 (2018) 160.



Event	Type	Mode	Sum. LIGO prob.	Obs. time	Upper limits	
					Ene. Flux $\text{erg cm}^{-2} \text{s}^{-1}$	Lum. erg s^{-1}
GW150914	BH-BH			Before operation		
GW151226	BH-BH	LE HXM SGM	15%	$T_0-525 - T_0+211$	9.3×10^{-8} 1.0×10^{-6} 1.8×10^{-6}	2.3×10^{48} $3-5 \times 10^{49}$
GW170104	BH-BH	HE	30%	$T_0-60 - T_0+60$	6.4×10^{-6}	6.2×10^{50}
GW170608	BH-BH	HE	0%	$T_0-60 - T_0+60$	Out of FOV	
GW170814	BH-BH	HE	0%	$T_0-60 - T_0+60$	Out of FOV	
GW170817	NS-NS	HE	0%	$T_0-60 - T_0+60$	Out of FOV	

- CALET can search for EM counterparts to LIGO/Virgo triggers
- All O1 and O2 triggers checked – no signal in CGBM or CAL
- Upper limits set for GW151226 for CGBM+CAL in 2016 paper
- Upper limits for the CAL set using refined LE selection for triggers to-date in the 2018 paper



CALET: Summary and Future Prospects

- ❑ CALET was successfully launched on Aug. 19th, 2015. The observation campaign started on Oct. 13th, 2015. Excellent performance and remarkable stability of the instrument.
- ❑ As of May 31, 2019 total observation time is 1327 days with live time fraction to total time close to 84%. Nearly 1.8 billion events collected with low (> 1 GeV) + high energy (>10 GeV) triggers.
- ❑ Accurate calibrations have been performed with non-interacting p & He events + linearity in the energy measurements established up to 10^6 MIP.
- ❑ Measurement of **electron+positron spectrum** in 11 GeV - 4.8 TeV range using full acceptance
Observation of a flux reduction above 1 TeV.
- ❑ Direct measurement of **proton spectrum** in 50 GeV – 10 TeV energy range. Spectral hardening observed above a few hundred GeV.
- ❑ Preliminary analysis of primary elements up to Fe and secondary-to-primary ratios.
- ❑ Preliminary analysis of UH cosmic rays up to $Z=40$.
- ❑ Study of diffuse and point sources with gamma-rays. Follow-up observations of GW events in X-ray and gamma-ray bands. CALET's CGBM detected 159 GRBs in the energy range 7 keV-20 MeV.
- ❑ After an initial period of 2 years CALET observation time has been extended to 5 years at least.



Lessons Learned in view of Next Gapes

The next generation of CR instruments should aim to fulfill (at least partially) the following:

① LARGE GEOMETRIC FACTOR

- next generation of 3-D calorimeters can reach $10 \text{ m}^2 \text{ sr}$

② EXCELLENT CHARGE IDENTIFICATION

- *redundant* charge identifiers to cross calibrate in flight against each other
- *ad hoc granularity* to reduce ambiguities due to backscattering (gets worse at higher energy)
- VERY large *dynamic range* to cover high-Z nuclei

③ TRACKING is ESSENTIAL

- cuts down systematics on geometric acceptance
- mitigates backscattering ambiguities in charge identification
- multi-track + vertex reconstruction improve systematics related to particle interactions

④ ENERGY MEASUREMENT, SCALE ASSESSMENT & PID

- thick calorimeter for shower containment ($30 X_0$ or more)
- VERY large *dynamic range* to reach PeV energies ($>10^6 \text{ mip}$)
- redundant energy measurements for cross calibration (e.g.: $\beta\gamma$ from TRD below saturation)

⑤ IMPROVEMENTS in HADRONIC MODELS and MC simulations

- CR community should foster significant improvements of GEANT4, FLUKA at high energy
- continue to push measurements of poorly known cross sections



CALET

Thank you
for your attention !



CALET Collaboration Team



O. Adriani²⁵, Y. Akaike², K. Asano⁷, Y. Asaoka^{9,31}, M.G. Bagliesi²⁹, E. Berti²⁵, G. Bigongiari²⁹,
W.R. Binns³², S. Bonechi²⁹, M. Bongio²⁵, P. Brogi²⁹, A. Bruno¹⁵, J.H. Buckley³², N. Cannady¹³,
G. Castellini²⁵, C. Checchia²⁸, M.L. Cherry¹³, G. Collazuol²⁶, V. Di Felice²⁸, K. Ebisawa⁸, H. Fuke⁸, T.G. Guzik¹³,
T. Hams³, N. Hasebe³¹, K. Hibino¹⁰, M. Ichimura⁴, K. Ioka³⁴, W. Ishizaki⁷, M.H. Israel³², K. Kasahara³¹,
J. Kataoka³¹, R. Kataoka¹⁷, Y. Katayose³³, C. Kato²³, Y. Kawakubo¹, N. Kawanaka³⁰, K. Kohri¹², H.S. Krawczynski³²,
J.F. Krizmanic², T. Lomtadze²⁷, P. Maestro²⁹, P.S. Marrocchesi²⁹, A.M. Messineo²⁷, J.W. Mitchell¹⁵, S. Miyake⁵,
A.A. Moiseev³, K. Mori^{9,31}, M. Mori²¹, N. Mori²⁵, H.M. Motz³¹, K. Munakata²³, H. Murakami³¹, S. Nakahira²⁰,
J. Nishimura⁸, G.A De Nolfo¹⁵, S. Okuno¹⁰, J.F. Ormes²⁵, S. Ozawa³¹, L. Pacini²⁵, F. Palma²⁸, V. Pal'shin¹,
P. Papini²⁵, A.V. Penacchioni²⁹, B.F. Rauch³², S.B. Ricciarini²⁵, K. Sakai³, T. Sakamoto¹,
M. Sasaki³, Y. Shimizu¹⁰, A. Shiomi¹⁸, R. Sparvoli²⁸, P. Spillantini²⁵, F. Stolzi²⁹, S. Sugita¹, J.E. Suh²⁹,
A. Sulaj²⁹, I. Takahashi¹¹, M. Takayanagi⁸, M. Takita⁷, T. Tamura¹⁰, N. Tateyama¹⁰, T. Terasawa⁷,
H. Tomida⁸, S. Torii^{9,31}, Y. Tunesada¹⁹, Y. Uchihori¹⁶, S. Ueno⁸, E. Vannuccini²⁵, J.P. Wefel¹³,
K. Yamaoka¹⁴, S. Yanagita⁶, A. Yoshida¹, and K. Yoshida²²

- 1) Aoyama Gakuin University, Japan
- 2) CRESST/NASA/GSFC and Universities Space Research Association, USA
- 3) CRESST/NASA/GSFC and University of Maryland, USA
- 4) Hirosaki University, Japan
- 5) Ibaraki National College of Technology, Japan
- 6) Ibaraki University, Japan
- 7) ICRR, University of Tokyo, Japan
- 8) ISAS/JAXA Japan
- 9) JAXA, Japan
- 10) Kanagawa University, Japan
- 11) Kavli IPMU, University of Tokyo, Japan
- 12) KEK, Japan
- 13) Louisiana State University, USA
- 14) Nagoya University, Japan
- 15) NASA/GSFC, USA
- 16) National Inst. of Radiological Sciences, Japan
- 17) National Institute of Polar Research, Japan

- 18) Nihon University, Japan
- 19) Osaka City University, Japan
- 20) RIKEN, Japan
- 21) Ritsumeikan University, Japan
- 22) Shibaaura Institute of Technology, Japan
- 23) Shinshu University, Japan
- 24) University of Denver, USA
- 25) University of Florence, IFAC (CNR) and INFN, Italy
- 26) University of Padova and INFN, Italy
- 27) University of Pisa and INFN, Italy
- 28) University of Rome Tor Vergata and INFN, Italy
- 29) University of Siena and INFN, Italy
- 30) University of Tokyo, Japan
- 31) Waseda University, Japan
- 32) Washington University-St. Louis, USA
- 33) Yokohama National University, Japan
- 34) Yukawa Institute for Theoretical Physics, Kyoto University, Japan



CALET Collaboration Team



O. Adriani²⁵, Y. Akaike², K. Asano⁷, Y. Asaoka^{9,31}, M.G. Bagliesi²⁹, E. Berti²⁵, G. Bigongiari²⁹,
W.R. Binns³², S. Bonechi²⁹, M. Bongio²⁵, P. Brogi²⁹, A. Bruno¹⁵, J.H. Buckley³², N. Cannady¹³,
G. Castellini²⁵, C. Checchia²⁶, M.L. Cherry¹³, G. Collazuol²⁶, V. Di Felice²⁸, K. Ebisawa⁸, H. Fuke⁸, T.G. Guzik¹³,
T. Hams³, N. Hasebe³¹, K. Hibino¹⁰, M. Ichimura⁴, K. Ioka³⁴, W. Ishizaki⁷, M.H. Israel³², K. Kasahara³¹,
J. Kataoka³¹, R. Kataoka¹⁷, Y. Katayose³³, C. Kato²³, Y. Kawakubo¹, N. Kawanaka³⁰, K. Kohri¹², H.S. Krawczynski³²,
J.F. Krizmanic², T. Lomtadze²⁷, P. Maestro²⁹, P.S. Marrocchesi²⁹, A.M. Messineo²⁷, J.W. Mitchell¹⁵, S. Miyake⁵,
A.A. Moiseev³, K. Mori^{9,31}, M. Mori²¹, N. Mori²⁵, H.M. Motz³¹, K. Munakata²³, H. Murakami³¹, S. Nakahira²⁰,
J. Nishimura⁸, G.A. De Nolfo¹⁵, S. Okuno¹⁰, J.F. Ormes²⁵, S. Ozawa³¹, L. Pacini²⁵, F. Palma²⁸, V. Pal'shin¹,
P. Papini²⁵, A.V. Penacchioni²⁹, B.F. Rauch³², S.B. Ricciarini²⁵, K. Sakai³, T. Sakamoto¹,
M. Sasaki³, Y. Shimizu¹⁰, A. Shiomi¹⁸, R. Sparvoli²⁸, P. Spillantini²⁵, F. Stolz²⁹, S. Sugita¹, J.E. Suh²⁹,
A. Sulaj²⁹, I. Takahashi¹¹, M. Takayanagi⁸, M. Takita⁷, T. Tamura¹⁰, N. Tateyama¹⁰, T. Terasawa⁷,
H. Tomida⁸, S. Torii^{9,31}, Y. Tunesada¹⁹, Y. Uchihori¹⁶, S. Ueno⁸, E. Vannuccini²⁵, J.P. Wefel¹³,
K. Yamaoka¹⁴, S. Yanagita⁸, A. Yoshida¹, and K. Yoshida²²

